AD-A031 354 IOWA UNIV IOWA CITY DEPT OF PHYSICS AND ASTRONOMY F/G 4/1
VLF EMISSIONS ASSOCIATED WITH ENHANCED MAGNETOSPHERIC ELECTRONS--ETC(U)
FEB 76 R R ANDERSON, K MAEDA N00014-76-C-0016
UNCLASSIFIED U. OF IOWA-76-8 NL

| OF |
AD A031354

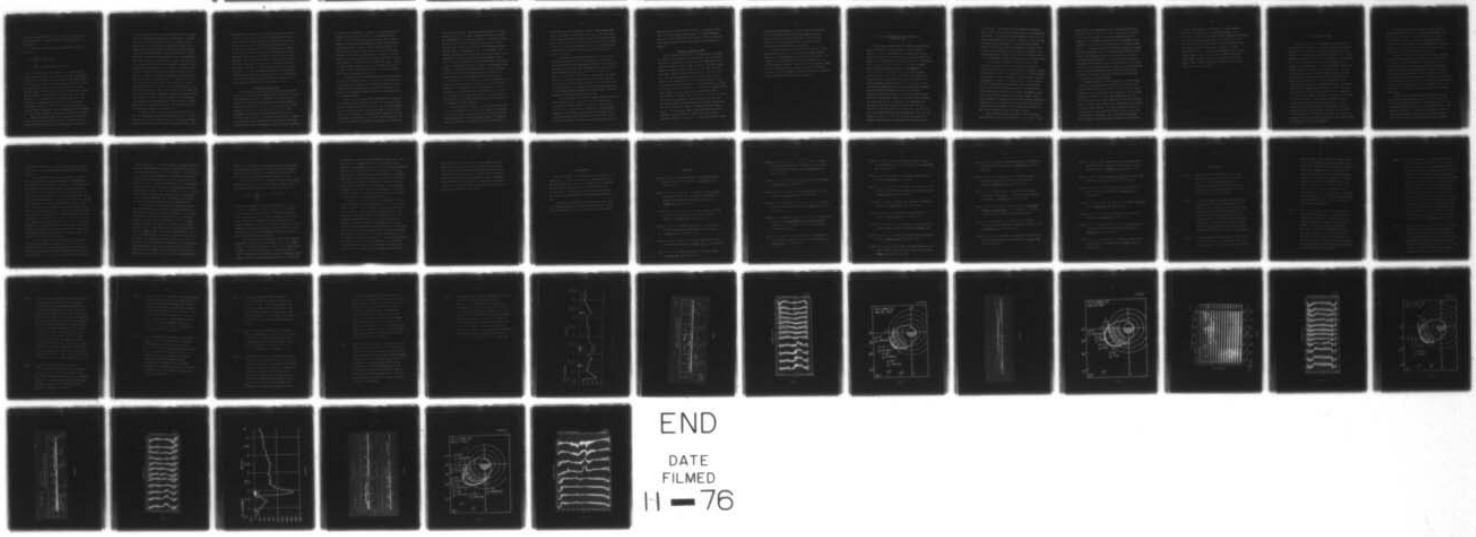

END

DATE FILMED
11-76

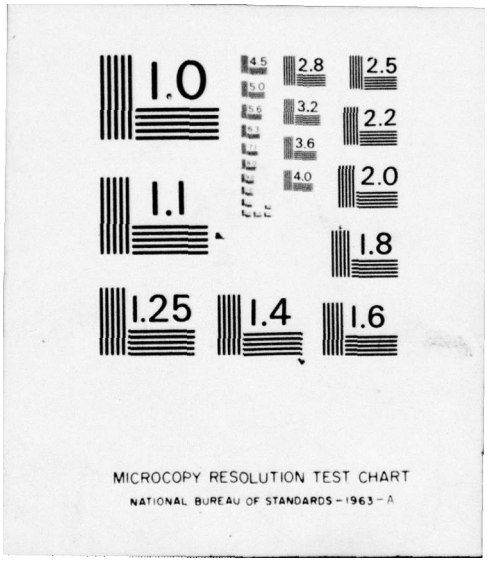
1.0
1.1
1.25
1.4
1.6
1.8
2.0
2.2
2.5
2.8
3.2
3.6
4.0
4.5
5.0
MICROCOPY RESOLUTION TEST CHART
NATIONAL BUREAU OF STANDARDS - 1963 - A

U. of Iowa 76-8

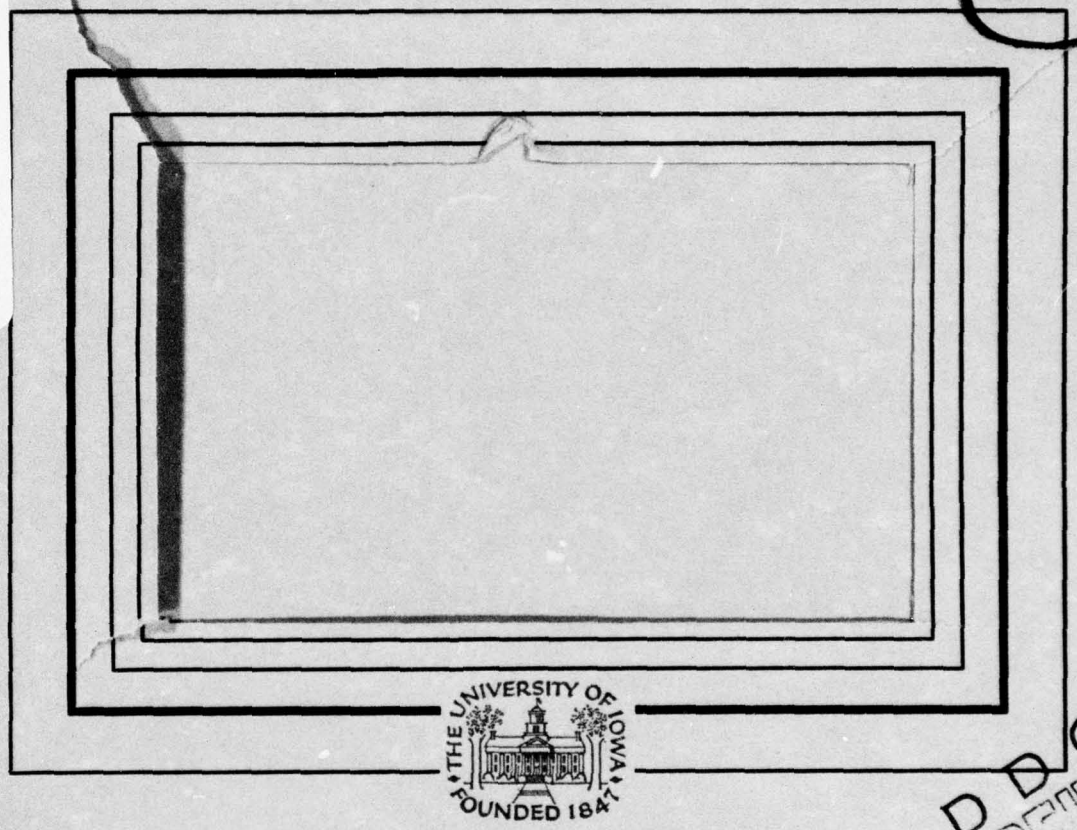

"Reproduction in whole or in part is permitted for any purpose of the United States Government. Research was supported in part by the Office of Naval Research under Contract N00014-76-C-0016."

Department of Physics and Astronomy

THE UNIVERSITY OF IOWA

Iowa City, Iowa 52242

U. of Iowa 76-8

VLF Emissions Associated with Enhanced Magnetospheric Electrons

by

Roger R. Anderson
Department of Physics and Astronomy
The University of Iowa
Iowa City, Iowa 52242

Kaichi Maeda
NASA/Goddard Space Flight Center
Greenbelt, Maryland 20771

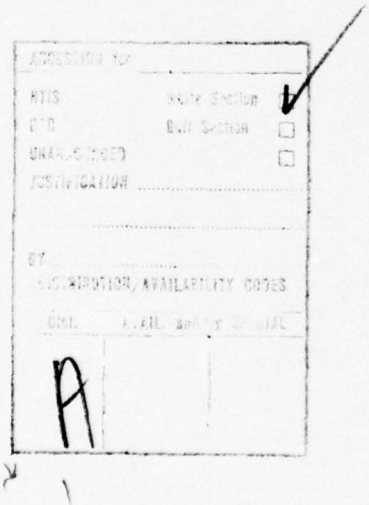

February, 1976

This research was supported in part by the National Aeronautics and Space Administration under Contract NAS5-11167 and Grant NGL-16-001-043 and the Office of Naval Research under Grant N00014-76-C-0016.

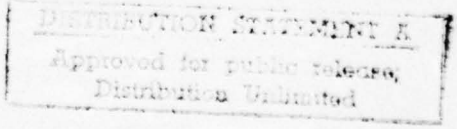

UNCLASSIFIED

SECURITY CLASSIFICATION OF THIS PAGE (When Data Entered)

REPORT DOCUMENTATION PAGE

READ INSTRUCTIONS BEFORE COMPLETING FORM

1. REPORT NUMBER

2. GOVT ACCESSION NO.

3. RECIPIENT'S CATALOG NUMBER

(rept.)

4. TITLE (and Subtitle)

(6) VLF Emissions Associated with Enhanced Magnetospheric Electrons.

5. TYPE OF REPORT & PERIOD COVERED

(9) Progress, February, 1976

6. PERFORMING ORG. REPORT NUMBER

(14) U. of Iowa-76-8

7. AUTHOR(s)

(10) Roger R. Anderson and Kaichi Maeda

8. CONTRACT OR GRANT NUMBER(s)

(15) N00014-76-C-0016
NAS5-11167

9. PERFORMING ORGANIZATION NAME AND ADDRESS

Department of Physics and Astronomy
The University of Iowa
Iowa City, Iowa 52242

10. PROGRAM ELEMENT, PROJECT, TASK AREA & WORK UNIT NUMBERS

11. CONTROLLING OFFICE NAME AND ADDRESS

(11) Office of Naval Research
Arlington, Virginia 22217

12. REPORT DATE

February, 1976

13. NUMBER OF PAGES

58

14. MONITORING AGENCY NAME & ADDRESS (if different from Controlling Office)

(12) 60pp.

15. SECURITY CLASS. (of this report)

UNCLASSIFIED

15a. DECLASSIFICATION/DOWNGRADING SCHEDULE

16. DISTRIBUTION STATEMENT (of this Report)

Approved for public release; distribution is unlimited.

17. DISTRIBUTION STATEMENT (of the abstract entered in Block 20, if different from Report)

18. SUPPLEMENTARY NOTES

To be published in J. Geophys. Res., 1976

19. KEY WORDS (Continue on reverse side if necessary and identify by block number)

VLF emissions

Enhanced Magnetospheric Electrons

20. ABSTRACT (Continue on reverse side if necessary and identify by block number)

[See page following]

DD FORM 1 JAN 73 1473 EDITION OF 1 NOV 68 IS OBSOLETE
S/N 0102-014-6601

UNCLASSIFIED

SECURITY CLASSIFICATION OF THIS PAGE (When Data Entered)

188 460

ABSTRACT

During periods of geomagnetic disturbances, VLF emissions and enhancements of low energy electrons are simultaneously observed by the equatorial orbiting ~~S-3-A~~ (Explorer 45) satellite. These events are characterized by the following features:--(i) The VLF emissions occur outside the plasmasphere in the nightside of the magnetosphere; (ii) The VLF emissions consist of two frequency regimes, one below the local electron gyrofrequency, f_{sub-g}, and the other above f_{sub-g}; (iii) The VLF emissions below f_{sub-g} are relatively broadband whistler-mode waves characteristic of chorus and frequently have a conspicuous band of missing emissions near $f_{sub-g}/2$. (iv) The emissions above f_{sub-g} are electrostatic and typically have components near $3f_{sub-g}/2$. Occasionally, higher frequency components are also observed; (v) The onset of the emissions coincides with abrupt increases outside the plasmasphere ($L \geq 4$) in 1 - 10 keV electrons to intensities of the order of 10^{8} electrons/cm^{2}/sec/ster/keV; Less pronounced enhancements sometimes occur for electrons with energies as high as 70 keV; and (vi) The cessation of the emissions coincides with a drop in the electron intensities to their pre-enhancement levels which are of the order of 10^{6} electrons/cm^{2}/sec/ster/keV or less. This drop in low energy electron intensities occurs before or when the satellite crosses the plasmapause back into the plasmasphere. These observed features

next pg

indicate that the VLF emissions are produced by low energy (1 - 10 keV) electrons which penetrate into the dusk-midnight sector of the magnetosphere from the geomagnetic tail during magnetic storms and substorms and drift eastwards outside the plasmasphere. In this paper, events observed during geomagnetically disturbed periods in December, 1971, and January, 1972, are discussed.

I. INTRODUCTION

The first high altitude satellite VLF experiment (OGO 1) indicated that the source of whistler-mode emissions in the magnetosphere lies close to the equatorial plane [Dunckel and Helliwell, 1969]. The equatorial enhancement of whistler-mode wave emissions has also been shown by Tsurutani and Smith [1974] by investigating the ELF data obtained by OGO 5. These investigations were, however, limited only to wave data. In this study, data from both the plasma wave experiment and the particle detector experiments on the equatorial orbiting S^3-A satellite are used to examine wave-particle interactions in the magnetosphere. The orbit of S^3-A (initial apogee is 5.24 R_E, perigee is 222 km, inclination is 3.6° and orbital period is 7 hr. 49 min.) plus an extensive set of field and particle experiments make the satellite particularly favorable for studies of wave-particle interactions in the magnetosphere [Longanecker and Hoffman, 1973]. The plasma wave experiment instrumentation consists of a 16-channel spectrum analyzer which covers the frequency range from 35 Hz to 100 kHz and a wideband AGC receiver with a bandpass from 100 Hz to 10 kHz [Anderson and Gurnett, 1973]. Both units are connected to a 5.08 meter tip-to-tip electric dipole antenna. The electron detection instrumentation used in this analysis consists of a cylindrical electrostatic analyzer-channel electron multiplier system measuring mean

energies from 1.2 keV to 26 keV in eight energy intervals [Longanecker and Hoffman, 1973] and a solid state detector with four levels having mean energies from 55 keV to 400 keV [Williams et al., 1974]. Supplementary data from the flux gate and search coil magnetometer experiments and the static electric field experiment are also used.

Plasma waves in the magnetosphere, their characteristics and occurrence as a function of location and geomagnetic activity and their interactions with energetic particles have been extensively studied by past experiments. First we shall briefly review past investigations of chorus and electrostatic ($f > f_g$) emissions, the two types of emissions with which this study is most concerned. Chorus is an electromagnetic emission with $f < f_g$ that consists of many randomly occurring discrete tones lasting a few tenths of a second that either rise or fall in frequency. In a morphological survey of VLF emissions observed with the low altitude Injun 3 satellite, Taylor and Gurnett [1968] found that for VLF emissions (primarily ELF hiss, chorus and VLF hiss) the region of most intense emissions moved to lower latitudes (which correspond to lower L-shells at the equator) during geomagnetically disturbed times. The Injun 3 VLF experiment used a magnetic loop antenna as a sensor. Similar results were obtained by Barrington et al. [1971] using Alouette 2 data. The Alouette 2 data was obtained using an electric dipole antenna as a sensor. Taylor and Gurnett [1968] also found that often chorus was confined to lower latitudes than ELF hiss. Russell et al. [1969] conducted a morphological study of ELF noise using data from the search coil magnetometer experiment on OGO 3. They concluded

that the source of burst-like noise was near the equator. Burtis and Helliwell [1969] reported observations of banded chorus in data from experiments using magnetic loop antennas on OGO 1 and OGO 3. Banded chorus is chorus that occurs in well defined frequency bands. The banded chorus was usually observed at L shells of 4 or greater which suggested that the noise was observed primarily outside the plasmasphere. Occurrence of the banded chorus was positively correlated with magnetic activity. In a companion study of magnetospheric whistler-mode emissions with the OGO 1 satellite Dunckel and Helliwell [1969] found that the upper-frequency limit of most of the observed emissions was proportional to the minimum electron gyrofrequency along the magnetic field line passing through the satellite. This was interpreted to mean that the source of the emissions lies close to the equatorial plane. Using OGO 5 search coil magnetometer data, Tsurutani and Smith [1974] studied ELF electromagnetic emissions in the midnight sector of the outer magnetosphere. They detected chorus in conjunction with magnetospheric substorms throughout the region from L = 5 to L = 9 but only during postmidnight hours. This chorus occurred most frequently at the geomagnetic equator and did not extend beyond $\pm$ 15° geomagnetic latitude. They found the distribution of chorus as a function of L and local time to be strikingly similar to the distribution of enhanced, trapped and precipitated substorm electrons with energies $>$ 40 keV. The postmidnight occurrence of the chorus was attributed to the eastward curvature and gradient drift of the injected electrons.

The first direct associations between whistler-mode waves and energetic particles were made at low altitudes. Oliven and Gurnett [1968] observed that microbursts of $E \geq 40$ keV electrons detected by the Injun 3 satellite were always accompanied by VLF chorus emissions. Using high altitude balloons launched from Siple station, Antarctica ($L = 4.2$) Rosenberg et al. [1971] observed one-to-one correlations between short bursts of $E > 30$ keV x-rays and bursts of VLF emissions at 2.5 kHz. The energy of the electrons contributing to the x-ray bursts was estimated to be 30 to 100 keV. Burton and Holzer [1974] in a study of chorus in the outer magnetosphere reported experimental support for the necessity of a critical pitch angle anisotropy for whistler-mode wave generation as proposed by Kennel and Petschek [1966]. On an OGO 5 pass through the nightside outer magnetosphere, Burton and Holzer [1974] observed that the region of maximum pitch angle anisotropy for 50 to 100 keV electrons coincided with the region of origin of chorus as identified by their wave normal analysis. Fredricks [1975] reviews some of the recent theoretical and experimental research regarding the association of chorus emissions and wave-particle interactions in the outer magnetosphere.

Intense magnetospheric electric field emissions near $3f_g/2$ were first observed by Kennel et al. [1970] on the OGO 5 satellite. These emissions were localized near the equator and were observed from 2100 to 1200 LT for $4 < L < 10$. Because of their high frequency and high electric field amplitudes (typically 1-10 mV m^{-1}), Kennel et al. [1970] suggested these emissions could be the source of strong

pitch angle diffusion and energization of 1-10 keV auroral zone electrons. Scarf et al. [1973] showed that enhanced levels for $f \geq 3f_g/2$ electric field emissions were associated with substorm expansions. They found post-expansion $f \simeq 3f_g/2$ waves to be intense enough to provide strong diffusion for $E > 50$-80 keV electrons and changes in the local pitch angle distributions were correlated with variations in wave amplitude levels. Electromagnetic chorus emissions were also observed during the substorm expansion phase, but they occurred later and with lower wave intensities than the $f \simeq 3f_g/2$ waves. Fredricks and Scarf [1973] using a more expanded set of OGO 5 data than Kennel et al. [1970] found that in the local time region from 1900 to 0700 LT the occurrence of emissions tended to be concentrated in the $5 \leq L \leq 7$ region. The emissions were also found to occur from +40° to -50° geomagnetic latitude. However the most intense $3f_g/2$ emissions were found near the geomagnetic equator and near local midnight which is the area at the base of the plasma sheet. Shaw and Gurnett [1975] have also observed $(n + 1/2)f_g$ electrostatic waves in the outer magnetosphere in data acquired using the long electric dipole antennas on IMP 6. Shaw and Gurnett [1975] suggested that the electrostatic noise bands they observed near the plasmapause were related to the upper hybrid resonance noise observed inside the plasmasphere and the $(n + 1/2)f_g$ waves observed in the outer magnetosphere.

II. MAGNETOSPHERIC VLF EMISSION EVENTS IN JANUARY, 1972

The hourly values of equatorial Dst [Sugiura and Poros, 1973] are plotted in Figure 1 for the period from January 21 to 26, 1972. Three shaded marks on the top of this figure indicate the duration of the VLF emission events observed by the S^3-A satellite during this geomagnetically-disturbed period which are discussed in this paper.

A. Orbit 211, January 22, 1972

On orbit 211, the satellite exited the plasmasphere at about 0514 UT (L = 4.19 and 18.0 hrs. MLT) and re-entered the plasmasphere about 0903 UT (L = 4.26 and 21.9 hrs. MLT). The times of plasmapause crossings used in this paper are all determined by the saturation of the onboard static electric field instrument [Maynard and Cauffman, 1973]. The VLF emission event began near apogee, well outside the main body of the plasmasphere. As shown in Figure 2, a whistler-mode emission known as chorus was first observed at 0704 UT (L = 5.16 and 20.0 hrs. MLT) and continued, although sometimes intermittently, until 0831 UT (L = 4.71, MLT = 21.3 hrs.). Figure 2 is a 0-10 kHz spectrogram of the electric field wideband data. This record displays the sharp band of "missing emissions" in the chorus near half the local electron gyrofrequency, $f_g/2$. Since the orbit is close to the magnetic equatorial plane, f_g can be regarded as being nearly equal to the equatorial electron gyrofrequency. In this paper the values for f_g are computed

from the local magnetic field measured by the onboard fluxgate magnetometer [L. J. Cahill, Jr., private communication, 1975]. Also evident in Figure 2 are the VLF emissions above f_g. A band of emissions whose frequency range extends from $\sim 1.25\ f_g$ to $\sim 1.50\ f_g$ is present from 0710 UT to 0822 UT. It will be shown in cases discussed later that these emissions with frequencies above f_g are electrostatic.

Electron intensities ($cm^{-2}\ sec^{-1}\ ster^{-1}\ keV^{-1}$) for electrons with mean energies from 1.2 keV up to 400 keV are shown in Figure 3, in which directional differential intensities for pitch angles $\sim 90°$ and $\sim 20°$ are plotted against UT by small x's and by closed circles, respectively. From this figure we can see that the VLF emissions are clearly related with the high intensity of electrons in the five lowest energy channels observed by this satellite (1.2 keV to 6.0 keV). The onset of the VLF emissions nearly coincides with the abrupt increase in the 1.2 keV electron intensities about 0700 UT. Both differential intensities are enhanced roughly 20 times from the pre-enhancement intensity of $10^6\ cm^{-2}\ sec^{-1}\ ster^{-1}\ keV^{-1}$ for small pitch angle electrons, and from $5 \times 10^6\ cm^{-2}\ sec^{-1}\ ster^{-1}\ keV^{-1}$ for 90°-pitch angle electrons, respectively. Successively higher energy electrons display somewhat later enhancements and lower overall intensities. At 6.0 keV, the intensities for both 20° and 90° pitch angles peak at $3 \times 10^6\ cm^{-2}\ sec^{-1}\ ster^{-1}\ keV^{-1}$ at about 0800 UT. No enhancement of electron intensities is observed above 6.0 keV. Around 0830 UT, the intensities for all five enhanced low energy electron channels begin dropping rapidly toward their pre-enhancement levels. This drop

in intensities coincides with the cessation of the VLF emissions and occurs approximately 30 minutes before the satellite re-enters the plasmasphere.

The energy of electrons in cyclotron resonance with whistler-mode waves is

$$E_c = E_B \frac{f_g}{f} \left(1 - \frac{f}{f_g}\right)^3 \text{ where}$$

$$E_B = \frac{B^2}{8\pi N} \text{ , the magnetic energy per particle.}$$

f is the wave frequency, B is the magnitude of the static magnetic field and N is the electron number density [Kennel and Petschek, 1966]. Between 0700 UT and 0800 UT, the static magnetic field remains within 10γ of 170γ [L. J. Cahill, Jr., private communication, 1975]. In this time period, electric field turbulence associated with the plasma frequency appears in the 16.5 kHz and 31.1 kHz channels of the on-board spectrum analyzer. This indicates the ambient number density was in the range of 4 to 10 electrons cm^{-3} [Gurnett and Shaw, 1973]. This implies that for whistler-mode waves with $f \simeq f_g/2$, the resonant energy ranges from 4.5 keV to 1.8 keV. Thus the energies where the electron intensity enhancements occur are appropriate for the electrons to be in cyclotron resonance with the observed whistler-mode emissions.

There are indications that near the beginning of the emission event, the satellite passed through several very narrow regions of plasma with densities comparable to the plasmasphere. From 0658 UT

to 0704 UT, 0705.5 UT to 0707.5 UT and 0718 UT to 0719 UT, the static electric field instrument briefly came out of saturation, indicating the local number density exceeded 40 cm^{-3} [N. C. Maynard, private communication, 1975]. VLF emissions associated with enhanced low energy electron intensities were not present for these time periods. Instead, a narrow electromagnetic band of hiss from 200 Hz to 500 Hz was observed. This ELF hiss band is characteristic of "plasmaspheric hiss" [Russell and Holzer, 1970; Carpenter, et al., 1969] which fills the plasmasphere but is believed to be generated just inside the plasmapause [Thorne et al., 1973]. In the low energy electron data, the intensities dropped briefly an order of magnitude near 0707 UT and 0718 UT. A diagram of the probable configuration of the evening plasmasphere for Orbit 211 is shown in Figure 4. Because of the presence of the plasmaspheric hiss we believe the high density cold plasma encountered around 0700 UT could be a tail-like extension from the main body of the plasmasphere. This narrow high density region shields the region outside the outbound plasmapause crossing from the enhanced low energy electrons. Possible tail-like extensions of the plasmasphere have been observed during geomagnetically disturbed times by Barfield et al. [1975] and Maynard and Chen [1975]. The location of the VLF emission event is indicated by the hatched line.

As shown in Figure 2, most of the wave energy from 0738 UT to 0801 UT is concentrated in the emissions above f_g which is ~ 4.8 kHz. From 0740 UT to 0750 UT the emissions appear in the spectrum analyzer channels up to 16.5 kHz. This indicates emissions up to $7f_g/2$. The

enhancement in the intensities of electrons with mean energies from 2.7 keV to 6.0 keV begins around 0730 UT and continues until about 0830 UT. The wave energy shifts to the whistler-mode emissions near $f_g/2$ at 0801 UT. At about the same time, as shown in Figure 3, the 90° pitch angle intensities for the 4.0 keV electrons drop around a half an order of magnitude. For the 6.0 keV electrons the 20° pitch angle intensities rise to a level slightly above 90° pitch angle intensities. Prior to this time, and for all lower energies, the 20° pitch angles were usually a half an order of magnitude below the 90° pitch angle intensities. At the termination of this emission event around 0831 UT, the 90° pitch angle intensities for all energies of electrons were greater than the corresponding 20° pitch angle intensities. The peak chorus amplitude measured during the period of the nearly isotropic pitch angle distributions was ~ 250 μV/m.

B. Orbit 214, January 23, 1972

The VLF emission event and low energy electron enhancement for Orbit 214 begin and end nearly coincident with the outbound and inbound bound plasmapause crossings. As determined by the saturation or the on-board static electric field instrument, the outbound plasmapause crossing occurs at 0424 UT (L = 4.17, MLT = 17.8 hrs.) and the inbound crossing is at 0852 UT (L = 3.52, MLT = 22.5 hrs.). A 0-10 kHz spectrogram of the electric field wideband data from 0400 UT to 0849 UT is shown in Figure 5. The wideband data end at 0849 UT because that is when the special purpose wideband transmitter was turned off. At 0426 UT, just outside the plasmapause, whistler-mode chorus emissions

with the sharp missing band at $f_g/2$ begin. These emissions are then present most of the time until 0524 UT. They reappear briefly at 0624 UT. From 0741 UT until the end of the data at 0849 UT they are present, although somewhat intermittently. Electric field emissions above f_g first appear in Figure 5 at 0431 UT and are evident until 0815 UT when they disappear because they are above the 10 kHz upper frequency cut-off of the wideband receiver. The electric field emissions above f_g in the wideband data have several bands which are each about 1 kHz wide. The most intense band appears near $3f_g/2$. At times the emissions extend almost as low as f_g. For example, near 0700 UT the lower cut-off of the emissions is about 4.8 kHz and the measured local electron gyrofrequency is 4.7 kHz.

The configuration of the plasmasphere near the evening quadrant for Orbit 214 is shown in Figure 6. The hatched lines indicate where the VLF emissions are observed. The plasmapause between the two orbit crossings is simply interpolated. The contracted plasmasphere is a result of the geomagnetic substorm indicated by the decreasing values of Dst shown in Figure 1.

Figure 7 is a plot of the digital output from the 16 channel onboard spectrum analyzer for the entire Orbit 214. The bottom channel covers the frequency range 100 Hz to 10 kHz. The next eleven channels, up to and including the 10 kHz channel, are connected to narrow-band filtes and have bandwidths $\pm$ 15% of their center frequencies. The top four channels have bandwidths $\pm$ 7.5% of their center frequencies. The output of each channel is approximately proportional to the logarithm

of the measured amplitude. The vertical lines represent the average amplitude measured over 64 second intervals of time and the dots are the peak amplitudes over the same time period. The baseline for each channel is about 2μV/m and full scale is about 20 mV/m. The low frequency signal present in the 35 Hz to 311 Hz channels from about 0300 UT to 0423 UT is plasmaspheric hiss. It also appears in the wideband spectrogram as the intense noise band near the bottom of the spectrogram. The abrupt termination of the plasmaspheric hiss at 0423 UT is also an indication of the outbound plasmapause crossing and is in good agreement with the static electric field plasmapause determination. The narrow noise band which peaks in the 100 kHz channel at 0420 UT and the 31.1 kHz channel at 0443 UT is similar to the plasma frequency noise band observed by Gurnett and Shaw [1973]. In the inbound portion of the orbit, this plasma frequency noise band peaks in the 31.1 kHz channel at 0838 UT and in the 100 kHz channel at 0855 UT. As the upper limit for the plasma density set by the saturation of the static electric field instrument is 60 ± 20 cm^{-3} [N. C. Maynard, private communication, 1975], the identification of this noise band as the plasma frequency noise band is consistent with the plasmapause crossing determination.

In the digital data in Figure 7, chorus is observed from 0426 UT to 0524 UT and from 0741 UT to 0852 UT. Because of its impulsive nature, chorus appears in the digital data with peak values usually much higher than their corresponding average values. The emissions above f_g are observed in the digital data from 0429 UT to 0856 UT,

shortly after the inbound plasmapause crossing. These emissions were usually the strongest in the channel nearest $3f_g/2$. The digital data also indicates emissions were present at higher half-integral harmonics of f_g. Between 0610 UT and 0700 UT, the emissions appeared very strong as high as 31.1 kHz which corresponds to 11 $f_g/2$. The peak amplitudes measured in this time interval ranged from .3 mV/m at 5.62 kHz to 1.4 mV/m at 31.1 kHz.

The directional differential intensities of 90° and 20° pitch angle electrons for Orbit 214 are plotted against time in Figure 8. Coincident with the outbound plasmapause crossing and the onset of the VLF emissions, the 90° pitch angle intensities for 1.2 keV to 1.8 keV electrons abruptly jump from 1.0×10^6 cm^{-2} sec^{-1} $ster^{-1}$ keV^{-1} to about 4.0×10^7 cm^{-2} sec^{-1} $ster^{-1}$ keV^{-1} at about 0425 UT. The intensities for 20° pitch angle electrons, which are near the loss cone, are about a half an order of magnitude lower. The 2.7 keV and 4.0 keV electron intensities also increased as the emission event progressed, but their enhancement was more gradual and somewhat less. Slight enhancements occurred later from 55 keV to 400 keV.

At 0500 UT where B was $\sim 215\gamma$, the resonant energy for whistler mode waves near $f_g/2$ is 2.9 keV if $N = 10$ cm^{-3}. Under the same conditions, the resonant energy for whistler-mode waves near 0.6 f_g and 0.4 f_g is 1.2 keV and 6.2 keV, respectively. Better agreement between the resonant energy required and the energy range where the greatest enhancement occurs requires N to be greater than 10 cm^{-3}. N could be increased by a significant contribution from the very low

energy part of the enhanced electron spectrum. It is worthy to note that in the wideband spectrogram in Figure 5, the chorus emissions above $f_g/2$ are more intense than those below $f_g/2$. This is consistent with enhanced cyclotron resonant interactions at the observed lower energies.

C. Orbit 220, January 25, 1972

The VLF emission event for Orbit 220 began shortly after apogee well outside the plasmasphere and terminated just after the satellite reentered the plasmasphere. The locations of the plasmapause and the observed VLF emission event are shown in Figure 9. The final outbound plasmapause crossing occurred at 0436 UT (L = 5.24, MLT = 19.6 hrs.) near apogee. Prior to this time, from 0259 UT (L = 4.41, MLT = 17.8 hrs.) on, the outer plasmasphere was rather tenuous and the static electric field instrument was at or near saturation much of the time. This detector came out of saturation on the inbound portion of the orbit at 0627 UT (L = 4.52, MLT = 20.6 hrs.). As shown in the wideband spectrogram in Figure 10, VLF emissions above f_g of moderate intensity (amplitudes up to 430 μV/m) began at 0517 UT (L = 5.18, MLT = 20.2 hrs.) well outside the plasmapause. Just prior to this time, very weak and barely discernable emissions above f_g were observed intermittently from 0448 UT to 0518 UT. However, their amplitudes never exceeded 40 μV/m. The VLF emissions above f_g were present until the inbound plasmapause crossing at 0627 UT. However, after 0548 UT their amplitudes dropped to 40 μV/m or less. Strong chorus emissions having

the distinctive missing gap at $f_g/2$ began at 0530 UT and ended at 0632 UT, five minutes after the inbound plasmapause crossing. For two intervals in this time period, 0538 UT to 0552 UT and 0618 UT ot 0624 UT, the chorus emissions were absent while the electrostatic mode emissions above f_g continued.

As shown in Figure 11, the electron flux in the three lowest energy channels (1.2 keV to 2.7 keV) increased abruptly beginning about 0517 UT, coincidently with the onset of the VLF emissions. The electron flux in these three channels remained enhanced until the inbound plasmapause crossing. The presence of the VLF emissions appears to be well correlated with the increase in flux of the low energy electrons. There is no apparent correlation between the VLF emissions and the electron flux above 4.0 keV for this orbit.

III. VLF EMISSION EVENT DURING DECEMBER, 1971, GEOMAGNETIC STORM

The VLF emission event for Orbit 101 occurred during the main phase of a geomagnetic storm on December 17, 1971, as shown in Figure 12. A 0-10 kHz spectrogram of the electric field wideband analog data from 1700 UT to 2200 UT and a 0-3 kHz spectrogram of the magnetic field wideband data are presented in Figure 13. VLF emissions above f_g began at 1717 UT (L = 4.45, MLT = 19.3 hrs.) coincident with the outbound plasmapause crossing. Electromagnetic chorus emissions with the missing gap at $f_g/2$ began 14 minutes later at 1731 UT (L = 4.66, MLT = 19.6 hrs.). Both chorus and the emissions above f_g were present until 2150 UT, just prior to the inbound plasmapause crossing at 2155 UT (L = 3.00, MLT = 0.2 hrs.). Although the emissions above f_g and the chorus emissions disappeared from the wideband spectrograms at about 2115 UT and 2145 UT, respectively, when they exceeded the 10 kHz upper cutoff frequency, both sets of emissions were present in the onboard spectrum analyzer data until about 2150 UT. The locations of the plasmapause and the observed VLF emission events are shown in Figure 14. From 1800 UT (L = 4.98, MLT = 20.0 hrs.) to 2005 UT (L = 5.00, MLT = 20.6 hrs.) the chorus emissions only had wave energy well below $f_g/2$. For example, at 1900 UT (L = 5.26, MLT = 20.8 hrs.) near apogee, the frequency range of the chorus emissions was 470 Hz to 730 Hz, i.e.,

0.12 to 0.18 f_g. It is evident from the wideband spectrograms in Figure 13 near 1950 UT that the emissions above f_g were predominantly electrostatic. In the electric field spectrogram, a narrow band of emissions was present at around 1950 UT just above 2.5 kHz, the measured local electron gyrofrequency. Even though these emissions occurred below the 3 kHz upper cutoff frequency of the search coil antennas, no emissions above f_g were observed in the magnetic field wideband spectrogram. Thus we conclude that the VLF emissions above f_g are electrostatic mode waves, as discussed previously [Maeda, 1976].

The directional differential intensities for 90° and 20° pitch angle electrons for Orbit 101 are presented in Figure 15. Coincident with the onset of the VLF emissions at the outbound plasmapause crossing at 1717 UT, the intensity of 1.8 keV electrons abruptly increased over two orders of magnitude. Shortly thereafter, similar enhancements were observed up through the 6.0 keV electron channel. All these low energy electron intensities remained enhanced until about 2150 UT when the VLF emissions ceased. Less abrupt and less intense enhancements occurred near the outbound plasmapause crossing for electrons with mean energies up to 100 keV. However, near the inbound plasmapause crossing, when the low energy electron intensities decreased and the VLF emissions ceased, the higher energy electron intensities remained enhanced. The VLF emissions thus appear to be most closely associated with the low energy electrons.

When the chorus emissions began near 1731 UT, the resonant energy for waves near $f_g/2$ was 1.8 keV for $N = 10\ cm^{-3}$ and $B = 180\gamma$.

Around 1950 UT, the resonant energy for the observed waves near $f_g/6$ was 7.0 keV for N = 10 cm^{-3} and B = 90γ. Waves near $f_g/2$ for similar N and B near 2010 UT would be in cyclotron resonance with 500 eV electrons. As the satellite continued inbound, the resonance energy, assuming N = 10 cm^{-3}, would have continued to climb to around 200 keV near L = 3. It appears that enhanced low energy electrons are required for the VLF emissions to occur. Near apogee where the magnetic field is small, the low energy electrons are the electrons in cyclotron resonance with chorus emissions. As the satellite moves inbound and the magnetic field increases, higher energy electrons are in cyclotron resonance with the chorus emissions. However, the low energy electrons must control the interaction because the emissions cease when the intensity of low energy electrons drops before the abrupt increase in number density at the plasmapause.

As shown in Figure 15, peculiar variations in the pitch angle distributions of high energy electrons from 400 keV down to 55 keV occurred from about 1800 UT to 2100 UT. First in the highest energy channel and later in successively lower channels, the 20° pitch angle intensities exceeded the 90° pitch angle intensities. And about 1855 UT near apogee, the overall intensities of high energy electrons abruptly increased, first in the 400 keV channel and later in successively lower energy channels. The electron intensities began to increase at 1905 UT, 1915 UT and 1920 UT for the 180 keV, 100 keV and 55 keV channels, respectively. These time delays are consistent with a localized injection of electrons earlier in local time than

S^3-A which drift eastward to the satellite. A substorm beginning about 1830 UT is indicated in the College magnetograms shown in Cahill [1973]. The time delays observed here are consistent with previous observations of Williams, et al. [1974]. In the 1800 UT to 2000 UT time period, the only noticeable change in the VLF emissions was that the chorus changed from having two bands near $f_g/2$ to a single emission band near $f_g/6$. This lower wave frequency requires a higher resonance energy, one at about 7 keV for the measured B-field and assumed number density. The unusual pitch angle distribution and abrupt increase in high energy electron intensities do not appear to affect the observed VLF emissions.

IV. DISCUSSION AND SUMMARY

This study has shown that magnetospheric VLF emissions with the characteristics listed below are clearly associated with enhanced intensities of low energy electrons which penetrate into the dusk-midnight sector of the magnetosphere from the geomagnetic tail during geomagnetic storms and substorms. The characteristics of the emissions are (i) the VLF emissions occur outside the plasmasphere in the nightside of the magnetosphere. (ii) The VLF emissions consist of two frequency regimes, one below f_g and the other above f_g. (iii) The VLF emissions below f_g are relatively broadband whistler-mode waves characteristic of chorus and frequently have a conspicuous band of "missing emissions" near $f_g/2$. (iv) The emissions above f_g are electrostatic and typically have components near $3f_g/2$. Occasionally, higher frequency components are also observed. (v) The onset of the emissions coincides with abrupt increases outside the plasmasphere ($L \geq 4$) in 1-10 keV electron intensities to the order of 10^8 electrons cm^{-2} sec^{-1} $ster^{-1}$ keV^{-1}. Less pronounced enhancements sometimes occur for electrons with energies as high as 70 keV. (vi) The cessation of the emissions coincides with a drop in the electron intensities to their pre-enhancement levels which are of the order of 10^6 electrons cm^{-2} sec^{-1} $ster^{-1}$ keV^{-1} or less. This drop in low energy electron intensities occurs before or when the satellite crosses the plasmapause back into the plasmasphere.

Calculations using the measured static magnetic field and a number density determined either by observed plasma frequency noise band or upper limits set by the static electric field instrument showed that the enhancements occurred at energies appropriate for electrons in cyclotron resonance with the observed whistler-mode wave frequencies. Little correlation was observed for electrons with energies above 70 keV and the observed VLF emissions.

Tsurutani and Smith [1974] suggested that a possible explanation for the "missing emissions" near $f_g/2$ might be Landau damping. For electrons in cyclotron resonance with waves at $f = f_g/2$, the parallel velocity of the electrons equals the wave phase velocity but the electrons are moving the opposite direction. Assuming that the electrons are moving along the field not bunched and in both directions, they noted that there would be electrons also moving in the same direction as the wave and with a velocity equal to the wave phase velocity. These electrons will Landau damp the wave provided they lie on a portion of the particle distribution function that is decreasing with energy.

Another possible explanation for the missing emission band that considers separate sources for the $f < f_g/2$ and $f > f_g/2$ has been proposed by Maeda et al. [1976]. They suggest that the $f > f_g/2$ emissions are generated locally near the satellite while the $f < f_g/2$ emissions are generated in a similar way but slightly outside the observing location where the local electron gyrofrequency would be lower. When these lower frequency emissions ultimately propagate

to the observing location via the ducted mode, their upper frequency cutoff will be one half the equatorial gyrofrequency of the observing location.

On a macroscopic scale, both chorus and the $f > f_g$ electrostatic emissions tended to occur coincident with the enhancement of the low energy electron intensities. However, on a microscopic scale the presence of one type of noise tended to quench the other type. For example on Orbit 214 from 0510 to 0525 UT in Figures 5 and 7 the chorus bursts occurred when the $f > f_g$ amplitudes decreased and chorus was absent when the strongest $f > f_g$ emissions occurred. This quenching effect was evident in the wideband spectrograms in Figures 2 and 10 also. However, some of the apparent quenching could have been due to the AGC of the wideband receiver. The amplitude at one frequency would appear weaker if a stronger signal at a different frequency occurred and controlled the receiver AGC. For Orbit 214 we were able to verify the quenching because it was also evident in the digital data. This verification is not usually possible or reliable unless the quenching effects are present for several sampling periods of the digital data. The interaction between the chorus and the electrostatic waves with $f > f_g$ will also be studied in future research.

On a given orbit, the chorus amplitudes tended to peak near where the maximum intensity of resonant electrons occurred. For instance on Orbit 220 the chorus amplitudes peaked at about 12.5 mV/m about 0555 UT, approximately the same time that the flux of 1.8 keV electrons peaked at 7.0×10^7 $(cm^2 \text{ sec ster})^{-1}$ and the flux of 2.7 keV

electrons peaked at 4.3×10^7 $(cm^2 \text{ sec ster})^{-1}$. Similarly on Orbit 214 the chorus amplitudes peaked at about 160 $\mu V/m$ when the flux of 4 keV electrons peaked at about 1.0×10^7 $(cm^2 \text{ sec ster})^{-1}$. On Orbit 220 the $f > f_g$ emissions had peak amplitudes of about 350 $\mu V/m$ around 0530 UT when the lowest energy electrons (1.2 keV) had a peak flux of 1.0×10^8 $(cm^2 \text{ sec ster})^{-1}$. However, for Orbit 214 the $f > f_g$ emissions had peak amplitudes up to 1.4 mV/m but the low energy electrons had peak fluxes of about 4.8 and 7.2×10^{-7} $(cm^2 \text{ sec ster})^{-1}$ for the 1.2 keV and 1.8 keV channels, slightly less than for Orbit 220. Quite possibly the $f > f_g$ emission amplitudes might be controlled by the electron spectrum below the lowest energy that could be measured on S^3-A.

To further test the plausibility of the low energy electrons interacting with the chorus via cyclotron resonance interactions we examined the relationship of the upper cutoff frequency of the chorus and anisotropy of the enhanced low energy electrons. For cyclotron resonance, the growth rate is proportional to a term $\left\{A - \frac{1}{f_g/f-1}\right\}$ [Kennel and Petschek, 1966] where A is a measure of the pitch angle anisotropy. From this expression we see that the growth rate goes to zero at $A = \frac{1}{f_g/f_c-1}$, where f_c is the upper cutoff frequency. For the cases we have examined in this study, f_c varied from about 0.55 f_g to 0.66 f_g. This corresponds to anisotropies of 1.22 to 1.94. The pitch angle plots of the resonant low energy electrons during periods of enhancement typically showed that the electron intensity varied from about $\sin^2 \alpha$ to $\sin^4 \alpha$ where α is the pitch angle. This indicates A ranges from 1 to 2 since for a pitch angle distribution proportional to

$\sin^m\alpha$, A = m/2. Occasionally the low energy electrons displayed pitch angle distributions proportional to sin α. The typical pitch angle distributions for the higher energy electrons varied from $\sin^{1/2}\alpha$ to sin α during the VLF emission events discussed in this study.

Kennel and Petschek [1966] calculated the maximum stably trapped omnidirectional flux, J*, for electrons above the resonance energy, E_R, in steady-state weak diffusion to be (within a factor of about 3)

$$J^*\ (>E_R) \approx \frac{1 - \frac{f}{f_g}}{A - \frac{1}{\frac{f_g}{f} - 1}} \cdot \frac{B}{L} \cdot 3 \times 10^{10}\ (\text{cm}^2\ \text{sec})^{-1}$$

where B is the equatorial field strength in Gauss. For $f = f_g/2$, A = 3/2, B = .002 Gauss, L = 5 and N = 10 cm^{-3}, $E_R \approx 2.5$ keV and $J^*\ (> 2.5\ \text{keV}) \approx 1.2 \times 10^7\ (\text{cm}^2\ \text{sec})^{-1}$. The low energy electron fluxes we observe during the VLF emission events are well above this level. However, as A approaches 1, the stably trapped flux limit increases dramatically. Near A = 1.1 the stably trapped flux limit is comparable to the low energy electron flux we have observed. Had the fluxes been less or had the anisotropies been smaller, we probably would not have observed chorus emissions.

Kennel et al. [1970] calculated that the pitch angle diffusion coefficient, D_α, associated with an electric field, E to be $\approx (\frac{eE}{mv})^2 \cdot \frac{1}{f}$ where v is the particle velocity and e and m are the charge and mass of electron. For 2 keV electrons and a 1 mV/m electric field, $D_\alpha \approx \frac{10^2}{f}$. For processes localized near the equator, Kennel et al. [1970] estimated that the electron encountered the wave electric field about

1% of the time. Thus the over-all diffusion coefficient for a 1 mV/m electric field is $\sim \frac{1}{f(\text{Hz})}$ $(\text{rad})^2$ sec^{-1}. In the examples we have discussed, f_g was typically around 5 kHz. Thus the diffusion coefficients would be 4×10^{-4} $(\text{rad})^2$ sec^{-1} and 1.3×10^{-4} $(\text{rad})^2$ sec^{-1} for $f_g/2$ and 3 $f_g/2$ waves, respectively, with 1 mV/m amplitudes. Scarf et al. [1973] loosely define strong diffusion to be above 10^{-3} $(\text{rad})^2$ sec^{-1}. Our calculations show that the observed 1 mV/m waves are around one half to one order of magnitude below that level. These calculations admittedly are fairly crude because of the assumptions on which they are based. However, the weaker waves with amplitudes of a few hundred μV/m most probably are in the weak diffusion regime.

Fredricks [1971] using a "ring" distribution showed that electrostatic fluctuations in the magnetosphere near $(n + 1/2)f_g$ could be produced by a peak in the perpendicular velocity distribution of the ambient electrons. Young et al. [1973] theoretically analyzed the generation of electrostatic waves in the magnetosphere using a more realistic distribution containing both a cold and warm species of electrons. They found the observed electrostatic spectra could be produced if the warm component had a non-zero peak in the perpendicular velocity distribution, if the density of the cold component was greater than about 1% of the warm and for high density regions if the cold to warm temperature ratio was not less than 0.1. Using differential energy flux data from De Forest and McIlwain [1971] from the geostationary ATS 5 satellite, Young et al. [1973] showed that a non-zero peak did exist in the perpendicular velocity distribution for electrons with

energy around 100 eV. Schield and Frank [1970] showed that at the inner edge of the plasma sheet around local midnight and near the equator there existed a peak in the differential energy spectra for electrons with energy of about 1 keV. Although we did not observe a peak in the low energy electron perpendicular velocity distribution associated with the electrostatic waves, the previous observations indicate such a peak probably existed for electrons less than the 1 keV minimum energy level that we could detect.

ACKNOWLEDGMENTS

We wish to thank Dr. R. A. Hoffman, Dr. D. J. Williams, Dr. D. A. Gurnett, Dr. L. J. Cahill, Jr., and Dr. N. C. Maynard for the use of their data in this study. We also wish to thank Mrs. Chris Gloeckler of GSFC, Dr. N. K. Bewtra of Computer Sciences Corporation, and Dr. Larry Lyons, Dr. Joe Barfield, and Mrs. Linda Bath of NOAA for their help in the computer analysis and preparation of the electron data.

This research was supported at the University of Iowa in part by the National Aeronautics and Space Administration under Contract NAS5-11167 and grant NGL-16-001-043 and the Office of Naval Research.

REFERENCES

Anderson, R. R. and D. A. Gurnett, Plasma wave observations near the plasmapause with the S^3-A satellite, J. Geophys. Res., 78, 4756-4764, 1973.

Barfield, J. N., J. L. Burch, and D. J. Williams, Substorm-associated reconfiguration of the dusk side equatorial magnetosphere: a possible source mechanism for isolated plasma regions, J. Geophys. Res., 80, 47-55, 1975.

Barrington, R. E., T. R. Hartz, and R. W. Harvey, Diurnal distribution of ELF, VLF, and LF noise at high latitudes as observed by Alouette 2, J. Geophys. Res., 76, 5278-5291, 1971.

Burtis, W. J. and R. A. Helliwell, Banded chorus - a new type of VLF radiation observed in the magnetosphere by OGO 1 and OGO 3, J. Geophys. Res., 74, 3002-3010, 1969.

Burton, R. K. and R. E. Holzer, The origin and propagation of chorus in the outer magnetosphere, J. Geophys. Res., 79, 1014-1023, 1974.

Cahill, L. J., Jr., Magnetic storm inflation in the evening sector, J. Geophys. Res., 78, 4724-4730, 1973.

Carpenter, D. L., C. G. Park, H. A. Taylor, Jr., and H. C. Brinton, Multi-experiment detection of the plasmapause from EOGO satellites and Antarctic ground stations, J. Geophys. Res., 74, 1837-1847, 1969.

De Forest, S. E. and C. E. McIlwain, Plasma clouds in the magnetosphere, J. Geophys. Res., 76, 3587-3611, 1971.

Dunckel, N. and R. A. Helliwell, Whistler-mode emissions on the OGO 1 satellite, J. Geophys. Res., 74, 6371-6385, 1969.

Fredricks, R. W., Plasma instability at $(n + 1/2)f_c$ and its relationship to some satellite observations, J. Geophys. Res., 76, 5344-5348, 1971.

Fredricks, R. W., Wave-particle interactions in the outer magnetosphere: a review, in The Magnetospheres of the Earth and Jupiter, V. Formisano, Ed., pp. 113-152, D. Reidel Publishing Company, Dordrecht-Holland, 1975.

Fredricks, R. W. and F. L. Scarf, Recent studies of magnetospheric electric field emissions above the electron gyrofrequency, J. Geophys. Res., 78, 310-314, 1973.

Gurnett, D. A. and R. R. Shaw, Electromagnetic radiation trapped in the magnetosphere above the plasma frequency, J. Geophys. Res., 78, 8136-8149, 1973.

Kennel, C. F. and H. E. Petschek, Limit on stably trapped particle fluxes, J. Geophys. Res., 71, 1-28, 1966.

Kennel, C. F., F. L. Scarf, R. W. Fredricks, J. H. McGehee, and F. V. Coroniti, VLF electric field observations in the magnetosphere, J. Geophys. Res., 75, 6136-6152, 1970.

Longanecker, G. W. and R. A. Hoffman, S^3-A spacecraft and experiment description, J. Geophys. Res., 78, 4711-4717, 1973.

Maeda, K., Cyclotron side-band emissions from magnetospheric electrons, Planet. Space Sci., 24, 341-347, 1976.

Maeda, K., P. H. Smith, and R. R. Anderson, VLF-emissions from ring current electrons, submitted for publication, Nature, 1976.

Maynard, N. C. and D. P. Cauffman, Double floating probe measurements on S^3-A, J. Geophys. Res., 78, 4745-4750, 1973.

Maynard, N. C. and A. J. Chen, Isolated cold plasma regions: observations and their relation to possible production mechanisms, J. Geophys. Res., 80, 1009-1013, 1975.

Oliven, M. N. and D. A. Gurnett, Microburst phenomena 3. An association between microbursts and VLF chorus, J. Geophys. Res., 73, 2355-2362, 1968.

Rosenberg, T. J., R. A. Helliwell, and J. P. Katsufrakis, Electron precipitation associated with discrete very-low-frequency emissions, J. Geophys. Res., 76, 8445-8452, 1971.

Russell, C. T., R. E. Holzer, and E. J. Smith, OGO 3 observations of ELF noise in the magnetosphere 1. Spatial extent and frequency of occurrence, J. Geophys. Res., 74, 755-777, 1969.

Russell, C. T. and R. E. Holzer, AC magnetic fields, in Particles and Fields in the Magnetosphere, B. M. McCormac, Ed., pp. 195-212, D. Reidel Publishing Company, Dordrecht-Holland, 1970.

Scarf, F. L., R. W. Fredricks, C. F. Kennel, and F. V. Coroniti, Satellite studies of magnetospheric substorms on August 15, 1968, J. Geophys. Res., 78, 3119-3130, 1973.

Schield, M. A. and L. A. Frank, Electron observations between the inner edge of the plasma sheet and the plasmasphere, J. Geophys. Res., 75, 5401-5414, 1970.

Shaw, R. R. and D. A. Gurnett, Electrostatic noise bands associated with the electron gyrofrequency and plasma frequency in the outer magnetosphere, J. Geophys. Res., 80, 4259-4271, 1975.

Sugiura, M. and D. J. Poros, Dst for 1971 and 1972, NASA-Goddard Space Flight Center, Greenbelt, Maryland 20771, April, 1973.

Taylor, W. W. L. and D. A. Gurnett, Morphology of VLF emissions observed with the Injun 3 satellite, J. Geophys. Res., 73, 5615-5626, 1968.

Thorne, R. M., E. J. Smith, R. K. Burton, and R. E. Holzer, Plasmaspheric hiss, J. Geophys. Res., 78, 1581-1596, 1973.

Tsurutani, B. T. and E. J. Smith, Postmidnight chorus: a substorm phenomenon, J. Geophys. Res., 79, 118-127, 1974.

Williams, D. J., J. N. Barfield, and T. A. Fritz, Initial Explorer 45 substorm observations and electric field considerations, J. Geophys. Res., 79, 554-564, 1974.

Young, T. S. T., J. D. Callen, and J. E. McCune, High-frequency electrostatic waves in the magnetosphere, J. Geophys. Res., 78, 1082-1099, 1973.

FIGURE CAPTIONS

Figure 1 Hourly values of the equatorial Dst (in γ) for the period from 1200 UT on January 21, 1972. to 1200 UT on January 26, 1972, [Sugiura and Poros, 1973]. The three shaded marks on the zero-line indicate the duration of the VLF emissions as observed by the S^3-A satellite during the orbits indicated.

Figure 2 A 0-10 kHz electric field wideband spectrogram of data observed by the S^3-A satellite during Orbit 211 on January 22, 1972. The whistler mode emissions with the conspicuous band of missing emissions near $f_g/2$ begin about 0704 UT with frequencies from 2 to 3 kHz and cease about 0831 UT. The higher frequency electrostatic emissions ($f > f_g$) begin about 0710 UT and cease about 0822 UT. The total duration of the enhanced low energy electron flux is indicated at the top of the spectrogram.

Figure 3 Variations of directional differential electron intensities (cm^{-2} sec^{-1} $ster^{-1}$ keV^{-1}) during the VLF-emission event on January 22, 1972. Small x's and closed circles

correspond to the intensities with pitch angles near 90° (78-90°) and the smallest observed pitch angles (22-34°), respectively. The time intervals indicated by horizontal hatched lines correspond to the periods when the VLF emissions are observed, and those of the shaded portions correspond to the inside of the plasmasphere. The mean energies of the electrons corresponding to each curve are from the bottom 1.2, 1.8, 2.7, 4.0, 6.0, 9.2, 13.5, 25.6, 55, 100, 180, and 400 keV, respectively. The measurements from 1.2 - 25.6 keV are made by a cylindrical electrostatic analyzer-channel electron multiplier system and the measurements from 55 - 400 keV are made with a solid state electron detector.

Figure 4 Orbit 211 of the S^3-A satellite. The hatched section along the orbit corresponds to the location where the VLF emissions are observed. The domain shaded in gray indicates the probable configuration of the evening plasmasphere. The satellite exited the plasmasphere at 0514 UT (L = 4.19 and 18.0 hrs. MLT) and re-entered the plasmasphere at 0903 UT (L = 4.26 and 21.9 hrs. MLT) as determined by the saturation of the onboard static electric field instrument. From 0658 to 0718 UT the satellite passed through several very narrow regions of plasma with densities comparable to the plasmasphere.

Figure 5 A 0-10 kHz spectrogram of the electric field wideband data for Orbit 214 on January 23, 1972. The whistler-mode chorus emissions with the sharp missing band begin just outside the outbound plasmapause crossing at 0424 UT and remain for about one hour. They begin again about 0741 UT and are present most of the time until the inbound plasmapause crossing at 0852 UT. The wideband data end at 0849 UT because that is when the special purpose wideband transmitter was turned off. The electrostatic emissions above f_g first appear at 0431 UT and are evident until 0815 UT when they disappear because they are above the 10 kHz upper cut-off frequency of the wide-band receiver. On this record, the most intense bands are near $3f_g/2$ but some of the electrostatic emissions extend almost as low as f_g. For example, near 0700 UT the lower cut-off of the emissions is about 4.8 kHz and the measured local electron gyrofrequency is 4.7 kHz.

Figure 6 Orbit 214 of the S^3-A satellite. The hatched area along the orbit shows the location of the VLF emissions and the shaded domain indicates the evening plasmasphere. The plasmapause between the two orbit crossings is simply interpolated. VLF emissions begin shortly after the outbound plasmapause crossing at 0424 UT (L = 4.17, MLT = 17.8 hrs.) and remain until the inbound plasmapause crossing at 0852 UT (L = 3.52, MLT = 22.5 hrs.).

Figure 7 A plot of the digital output from the 16 channel onboard spectrum analyzer for Orbit 214. The bottom channel is wideband and covers the frequency range from 0.1 to 10.0 kHz and the remaining 15 narrowband channels have center frequencies from 35 Hz to 100 kHz. The output of each channel is approximately logarithmically proportional to the measured amplitude. The vertical lines represent the average amplitude measured over 64 second intervals of time and the dots are peak amplitudes over the same time period. The baseline for each channel is about 2 μV/m and full scale is about 20 mV/m. PP indicates the plasmapause locations. The dashed lines labeled f_g and $2f_g$ indicate the location of the first and second harmonics of the electron gyrofrequency. The dashed line labeled f_p indicates the location of the electron plasma frequency. Note that near apogee, the electrostatic noise extends as high as 31.1 kHz which corresponds to $\sim 11\ f_g/2$.

Figure 8 Directional differential electron intensities ($cm^{-2}\ sec^{-1}\ ster^{-1}\ keV^{-1}$) during the VLF-emission event on January 23, 1972. Notations and energies of each curve are the same as those in Figure 3. The VLF-emission event and the low energy electron enhancement begin and end nearly coincident with the outbound and inbound plasmapause crossings, respectively.

Figure 9 Orbit 220 of the S^3-A satellite. The hatched area along the orbit shows the location of the VLF emissions. The shaded area indicates the equatorial cross-section of the evening plasmasphere. The final outbound plasmapause crossing occurs at 0436 UT (L = 5.24, MLT = 19.6 hrs.). Prior to this time, from 0259 UT (L = 4.41, MLT = 17.8 hrs.) on, the outer plasmasphere is rather tenuous. The inbound plasmapause crossing is at 0627 UT (L = 4.52, MLT = 20.6 hrs.). VLF emissions are observed from 0517 UT until 0632 UT.

Figure 10 A 0-10 kHz spectrogram of the electric field wideband data for Orbit 220 on January 25, 1972. Moderately intense electrostatic emissions above f_g begin at 0517 UT. Strong chorus emissions having the distinctive gap at $f_g/2$ begin at 0530 UT and end at 0632 UT. As shown at the top of the spectrogram, the enhanced low energy electron flux occurrence is nearly coincident with the presence of the VLF emissions. The location of the apogee and the outbound and inbound plasmapause crossings are indicated by arrows at the bottom of the spectrogram.

Figure 11 Directional differential electron intensities ($cm^{-2} sec^{-1} ster^{-1} keV^{-1}$) during the VLF-emission event on January 25, 1972. Notations and energies of each curve are the same as those in Figure 3 and 8. Note that the abrupt increase in low energy (1.2-2.7 keV) electron flux and the coincident onset of VLF emissions occur about 40 minutes after the outbound plasmapause crossing.

Figure 12 Hourly values of the equatorial Dst (in γ) for the period from December 16 to December 21, 1971, [Sugiura and Poros, 1973]. The shaded mark on the zero-line indicates the time of the VLF-emission event observed by the S^3-A satellite on Orbit 101 during the main phase of the December 17, 1971 geomagnetic storm.

Figure 13 Magnetic and electric field wideband spectrograms from 1700 UT to 2200 UT on December 17, 1971. The top record of each set contains the 0-3 kHz magnetic field wideband data from the search coil experiment. The lower record in each set contains the 0-10 kHz electric field wideband data. Electrostatic VLF emissions above f_g begin at the outbound plasmapause crossing at 1717 UT and last until they exceed the 10 kHz upper cutoff frequency of the electric field wideband data about

2115 UT. That these emissions are electrostatic can be seen in the data around 1950 UT where f_g is ~ 2.5 kHz. Emissions between 2.5 and 3.0 kHz are observed in the electric field wideband data but none are present in the magnetic field wideband data. Electromagnetic chorus emissions with the missing gap at $f_g/2$ begin at 1731 UT and are present until they exceed the upper cutoff frequencies of the wideband receivers. In the onboard spectrum analyzer data, both the emissions above and below f_g are present until 2150 UT. The VLF emissions were coincident with the enhancement of the low energy electron flux from 1717 UT to 2150 UT.

Figure 14 Orbit 101 of the S^3-A satellite. The hatched area along the orbit shows the location of the VLF emissions. The shaded area indicates the equatorial cross-section of the evening plasmasphere. The final sharp outbound plasmapause crossing is at 1717 UT, coincident with the onset of the VLF emissions and the enhancement of the low energy electron flux. The inbound plasmapause crossing at 2155 UT occurs just after the VLF emissions cease and the low energy electron enhancement stops. The plasmasphere is severely contracted as a result of the strong geomagnetic storm occurring.

Figure 15 Directional differential electron intensities (cm^{-2} sec^{-1} $ster^{-1}$ keV^{-1}) during the VLF-emission event on December 17, 1971. Notations are the same as those for Figures 3, 8, and 11. The onset and the end of the low energy electron enhancement coincide with the onset and end of the VLF emissions. The higher energy particles injected beginning about 1855 UT and the unusual pitch angle distributions for the higher energy particles from 1800 to 2100 UT appear to have little relation to the observed VLF emissions. The mean energies of the electrons corresponding to each curve are from the bottom 1.8, 2.7, 4.0, 6.0, 55, 100, 180, and 400 keV, respectively.

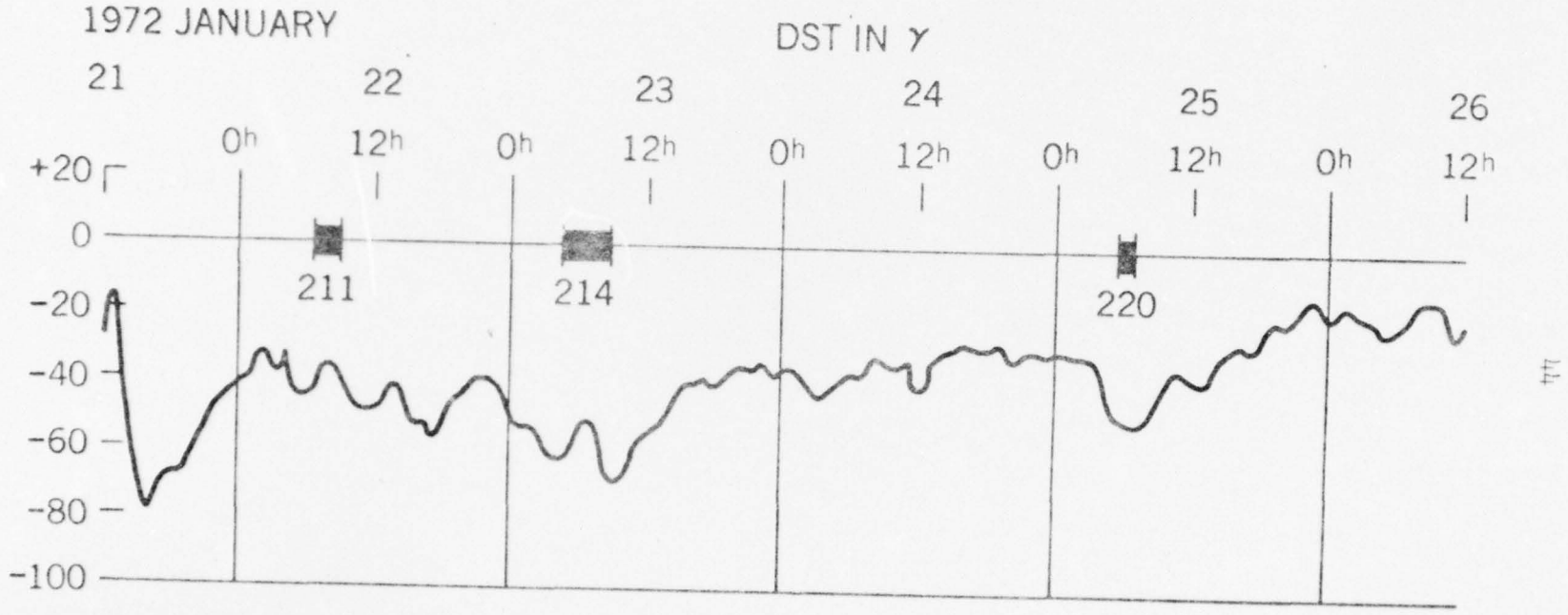
1972 JANUARY
DST IN γ
21
22
23
24
25
26
0h
12h
+20
0
-20
-40
-60
-80
-100
211
214
220

Figure 1

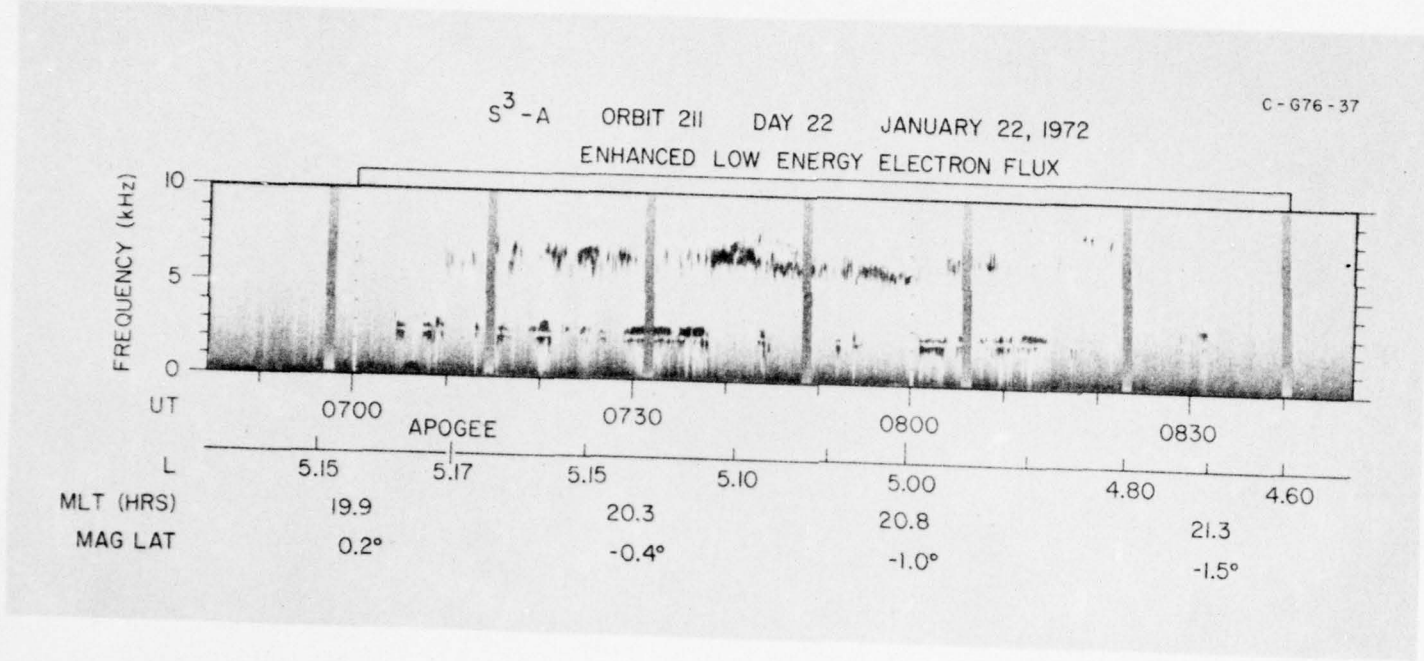
S3-A ORBIT 211 DAY 22 JANUARY 22, 1972
C-G76-37
ENHANCED LOW ENERGY ELECTRON FLUX
FREQUENCY (kHz)
10
5
0
UT
0700
APOGEE
0730
0800
0830
L
5.15
5.17
5.15
5.10
5.00
4.80
4.60
MLT (HRS)
19.9
20.3
20.8
21.3
MAG LAT
0.2°
-0.4°
-1.0°
-1.5°

Figure 2

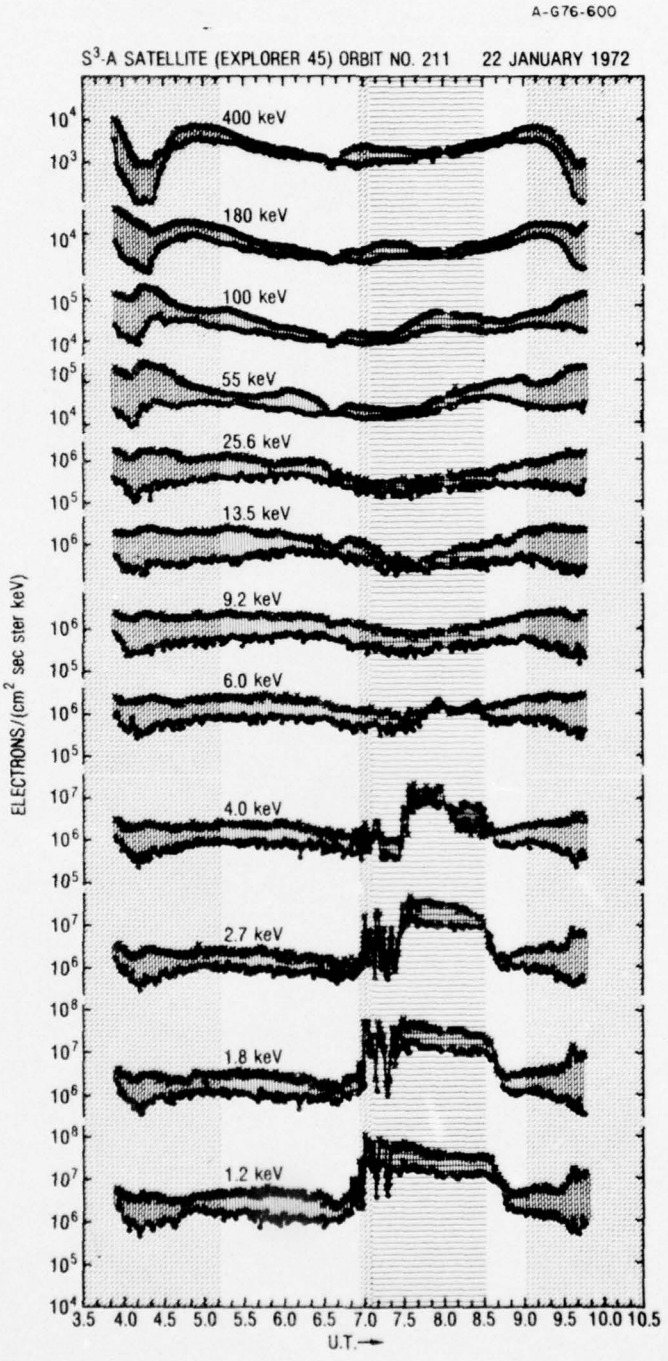
A-G76-600
S3-A SATELLITE (EXPLORER 45) ORBIT NO. 211 22 JANUARY 1972
400 keV
180 keV
100 keV
55 keV
25.6 keV
13.5 keV
9.2 keV
6.0 keV
4.0 keV
2.7 keV
1.8 keV
1.2 keV
ELECTRONS/(cm2 sec ster keV)
U.T.
3.5 4.0 4.5 5.0 5.5 6.0 6.5 7.0 7.5 8.0 8.5 9.0 9.5 10.0 10.5

Figure 3

A-G76-50-2

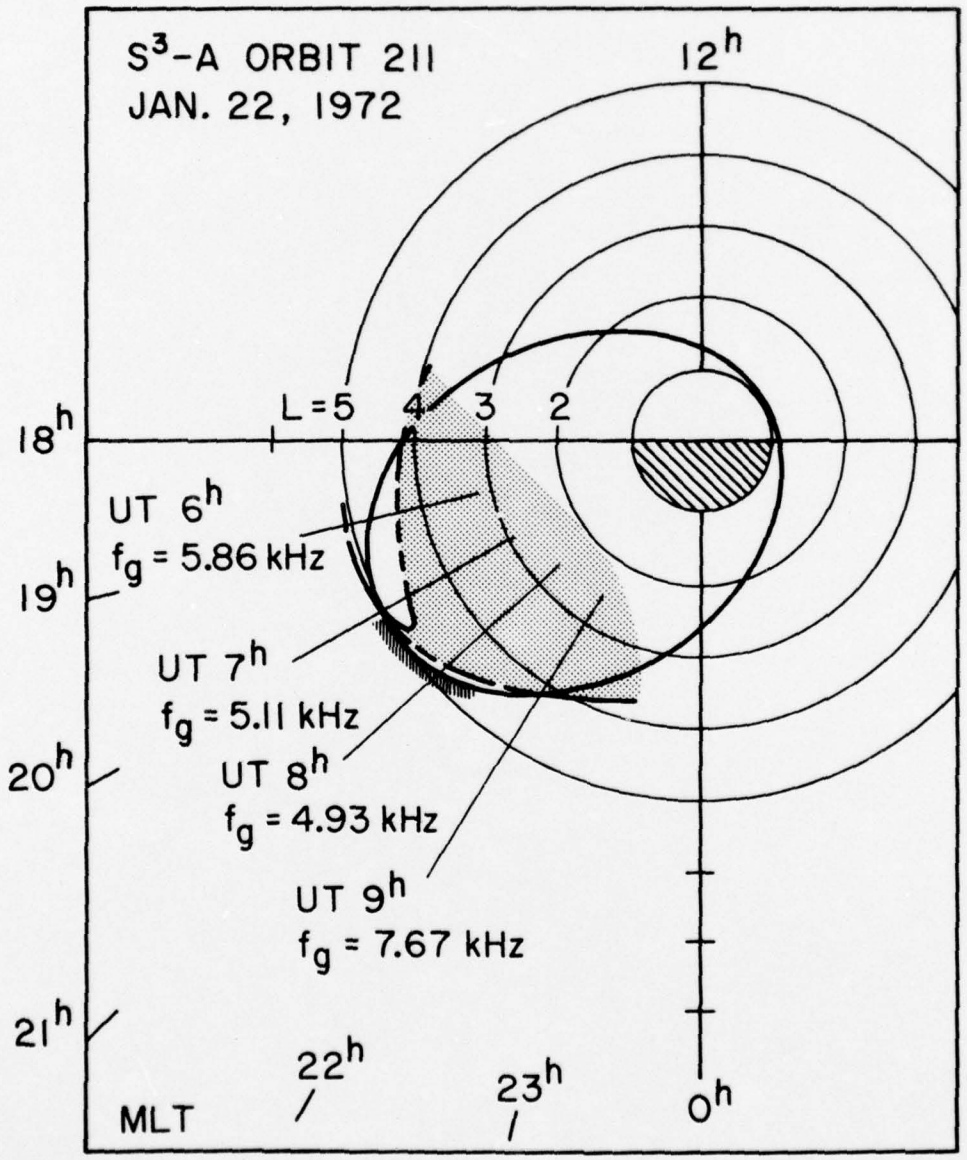

Figure 4

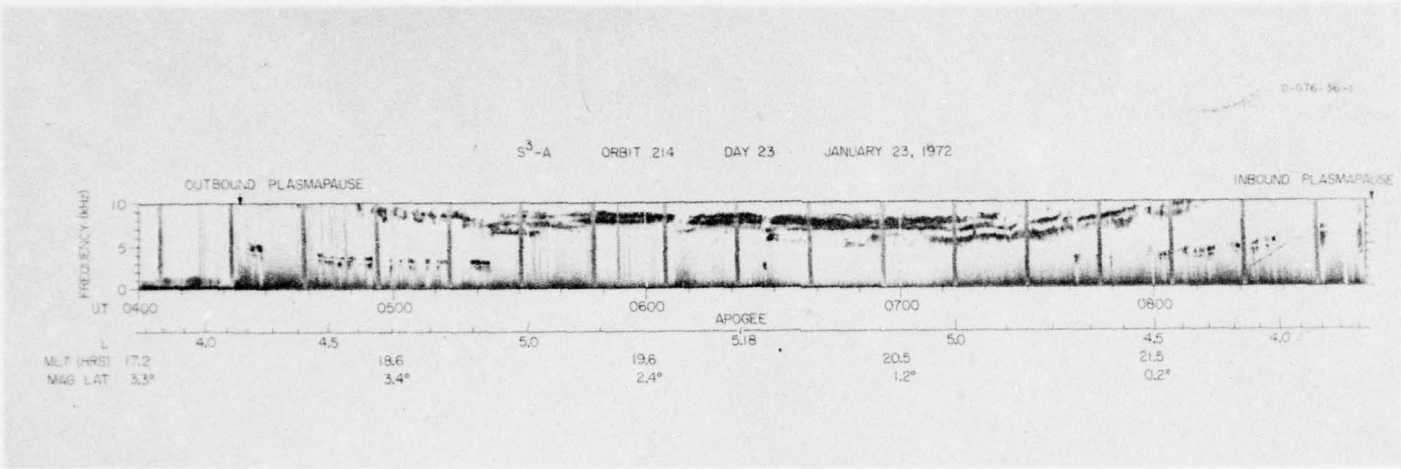
S3-A ORBIT 214 DAY 23 JANUARY 23, 1972
OUTBOUND PLASMAPAUSE
INBOUND PLASMAPAUSE
FREQUENCY (kHz)
10
5
0
UT 0400 0500 0600 0700 0800
APOGEE
L 4.0 4.5 5.0 5.18 5.0 4.5 4.0
MLT (HRS) 17.2 18.6 19.6 20.5 21.5
MAG LAT 3.3° 3.4° 2.4° 1.2° 0.2°

Figure 5

A-G76-51

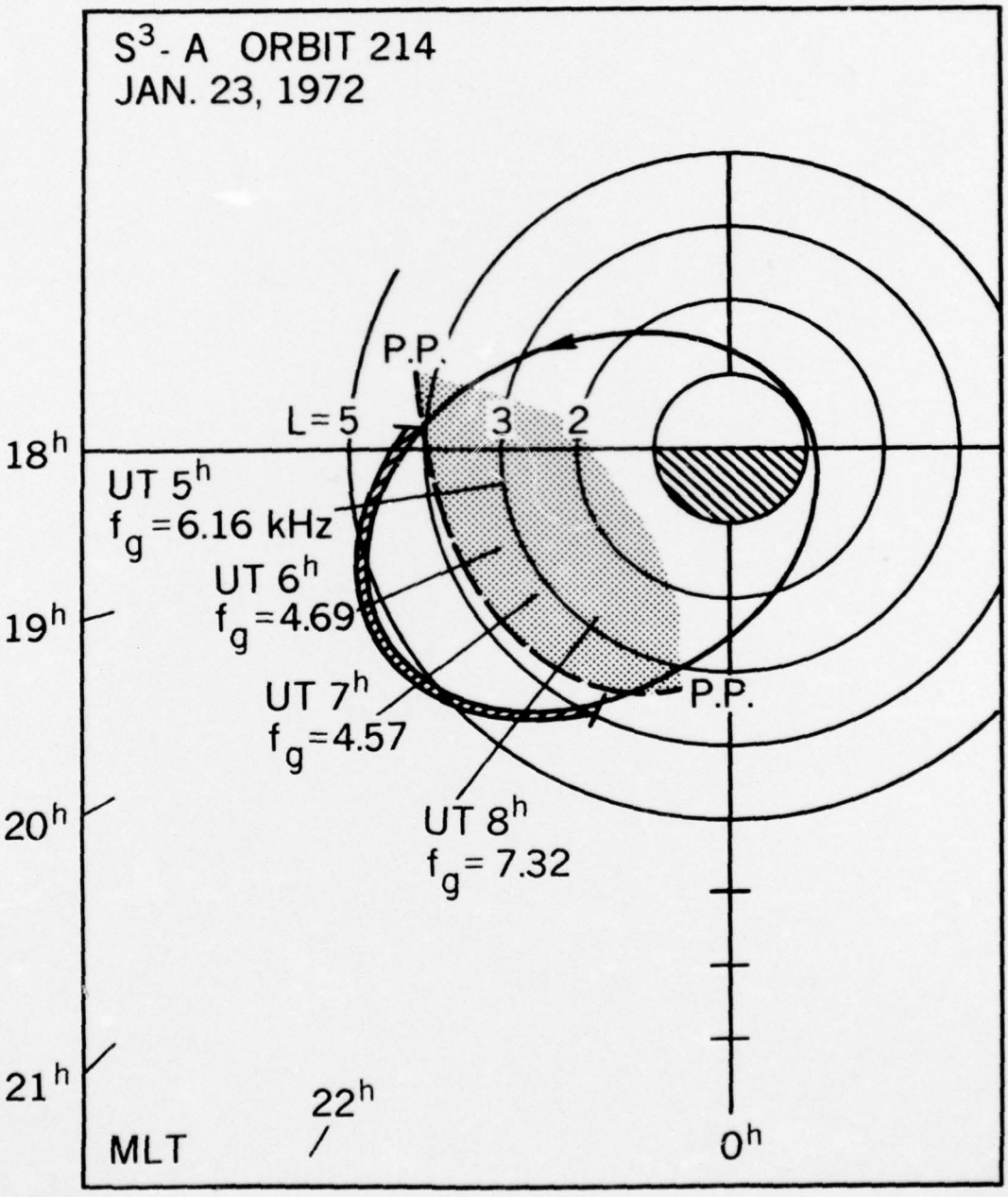

Figure 6

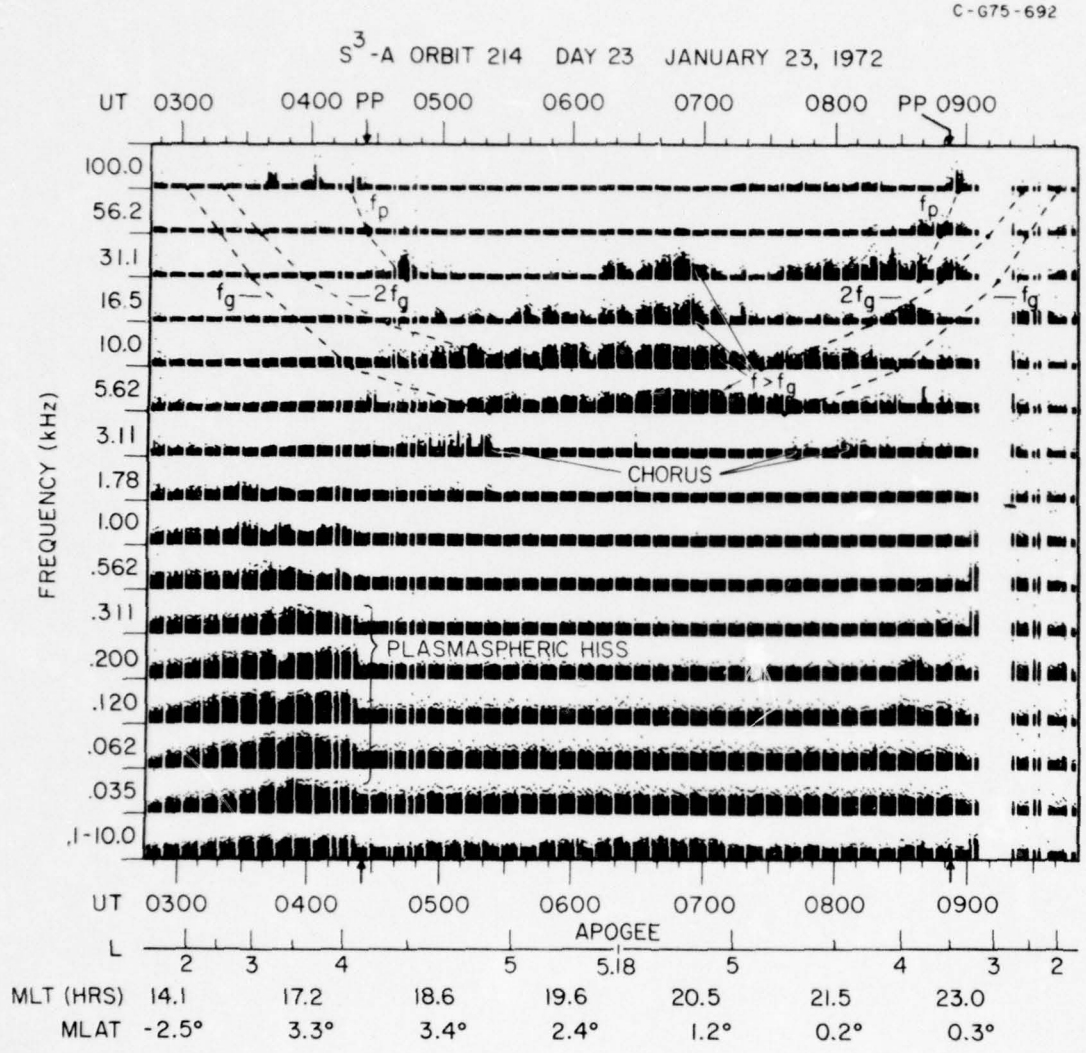
C-G75-692
S3-A ORBIT 214 DAY 23 JANUARY 23, 1972
UT 0300 0400 PP 0500 0600 0700 0800 PP 0900
FREQUENCY (kHz)
100.0
56.2
31.1
16.5
10.0
5.62
3.11
1.78
1.00
.562
.311
.200
.120
.062
.035
.1-10.0
fp
fg
2fg
f>fg
CHORUS
PLASMASPHERIC HISS
UT 0300 0400 0500 0600 0700 0800 0900
APOGEE
L 2 3 4 5 5.18 5 4 3 2
MLT (HRS) 14.1 17.2 18.6 19.6 20.5 21.5 23.0
MLAT -2.5° 3.3° 3.4° 2.4° 1.2° 0.2° 0.3°

Figure 7

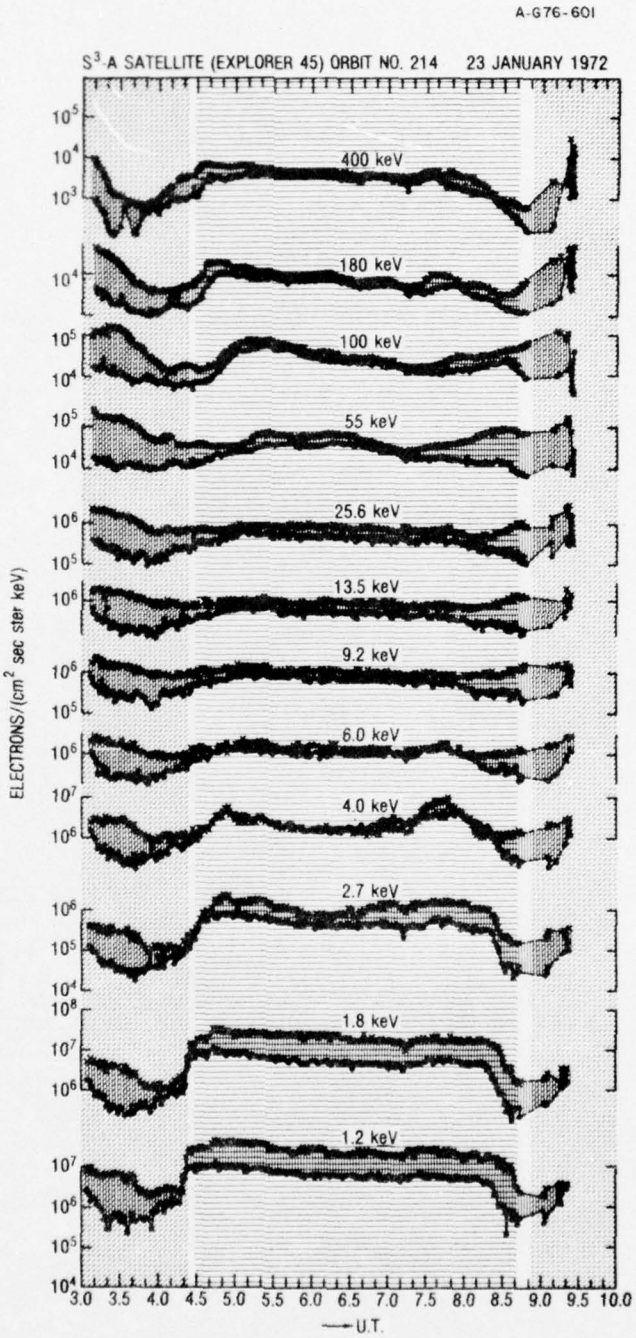
A-G76-601
S³-A SATELLITE (EXPLORER 45) ORBIT NO. 214 23 JANUARY 1972
400 keV
180 keV
100 keV
55 keV
25.6 keV
13.5 keV
9.2 keV
6.0 keV
4.0 keV
2.7 keV
1.8 keV
1.2 keV
ELECTRONS/(cm² sec ster keV)
3.0 3.5 4.0 4.5 5.0 5.5 6.0 6.5 7.0 7.5 8.0 8.5 9.0 9.5 10.0
U.T.

Figure 8

A-G76-52-1

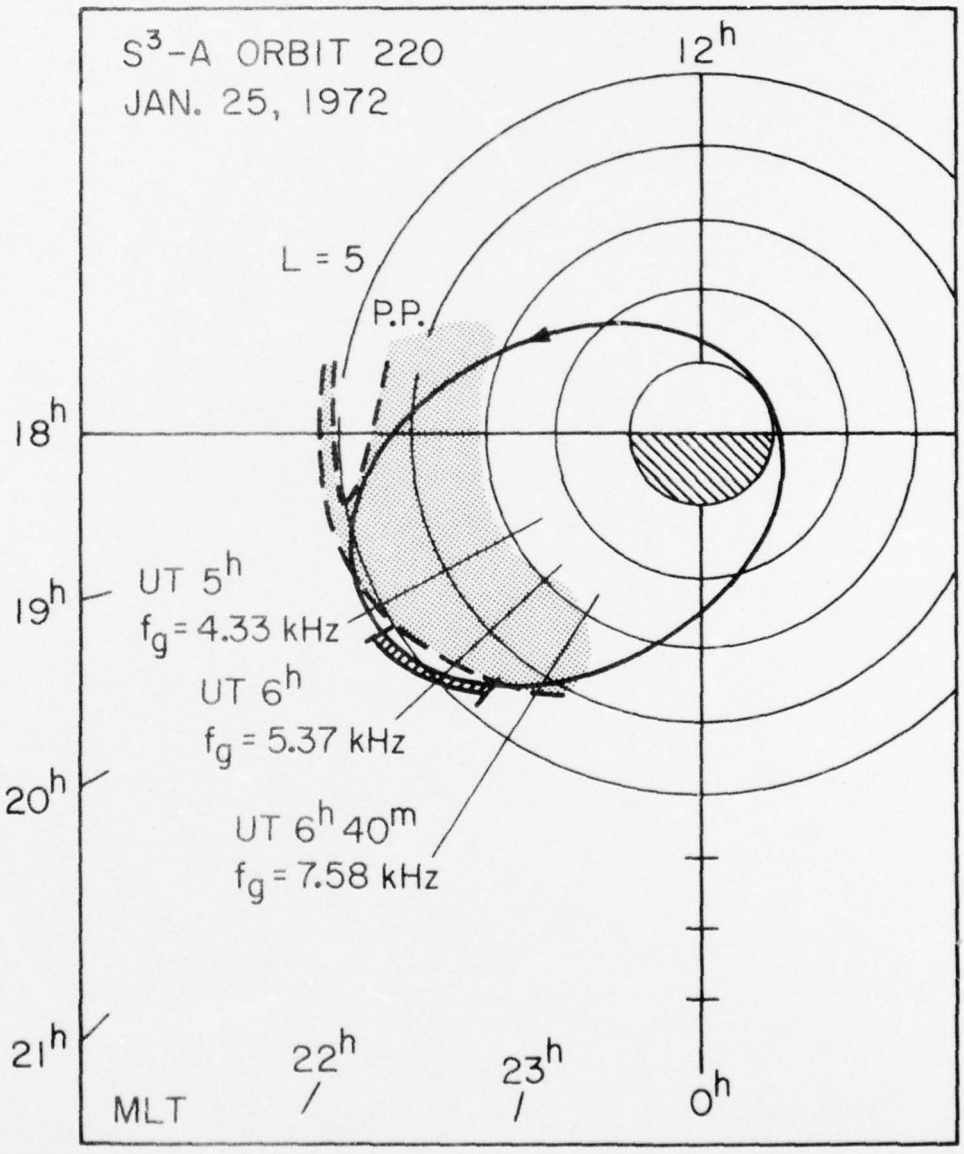

Figure 9

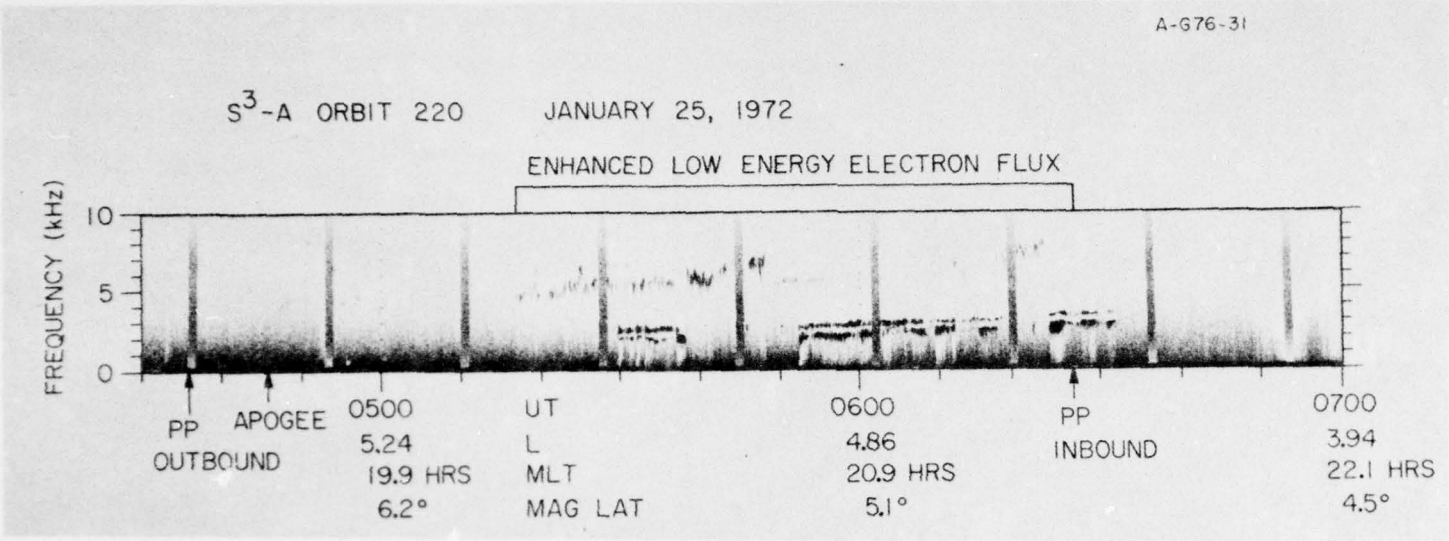
A-G76-31
S3-A ORBIT 220 JANUARY 25, 1972
ENHANCED LOW ENERGY ELECTRON FLUX
FREQUENCY (kHz)
10
5
0
PP
OUTBOUND
APOGEE
0500
5.24
19.9 HRS
6.2°
UT
L
MLT
MAG LAT
0600
4.86
20.9 HRS
5.1°
PP
INBOUND
0700
3.94
22.1 HRS
4.5°

Figure 10

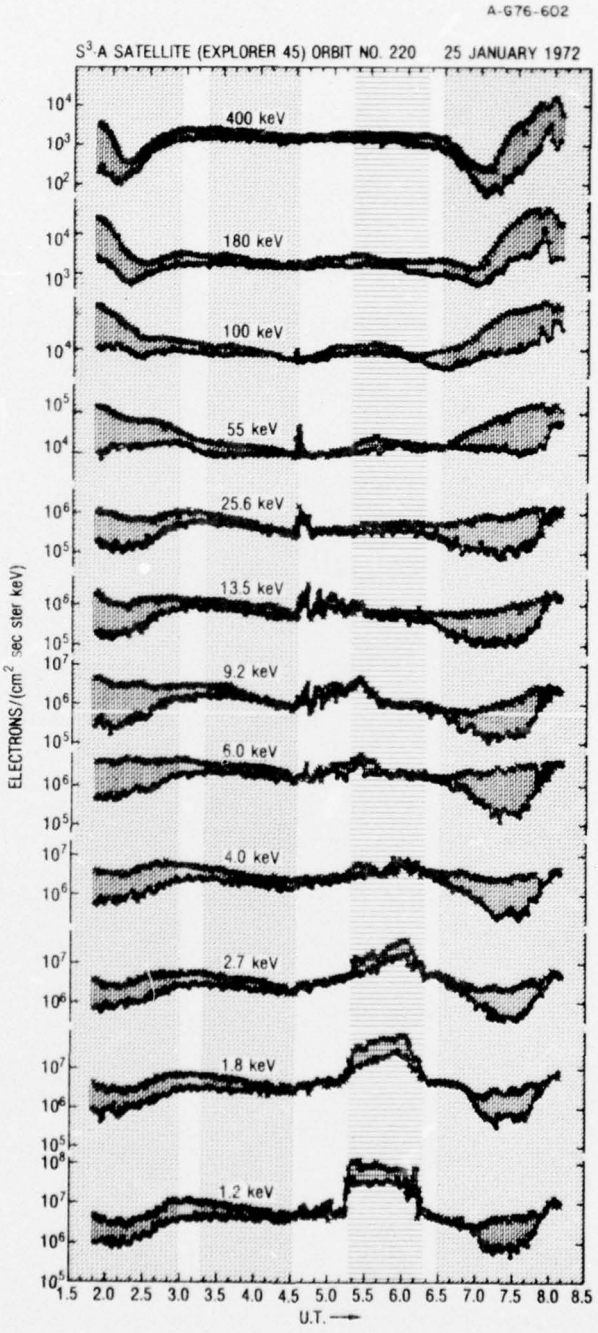
A-G76-602
S³-A SATELLITE (EXPLORER 45) ORBIT NO. 220 25 JANUARY 1972
400 keV
180 keV
100 keV
55 keV
25.6 keV
13.5 keV
9.2 keV
6.0 keV
4.0 keV
2.7 keV
1.8 keV
1.2 keV
ELECTRONS/(cm² sec ster keV)
1.5 2.0 2.5 3.0 3.5 4.0 4.5 5.0 5.5 6.0 6.5 7.0 7.5 8.0 8.5
U.T.

Figure 11

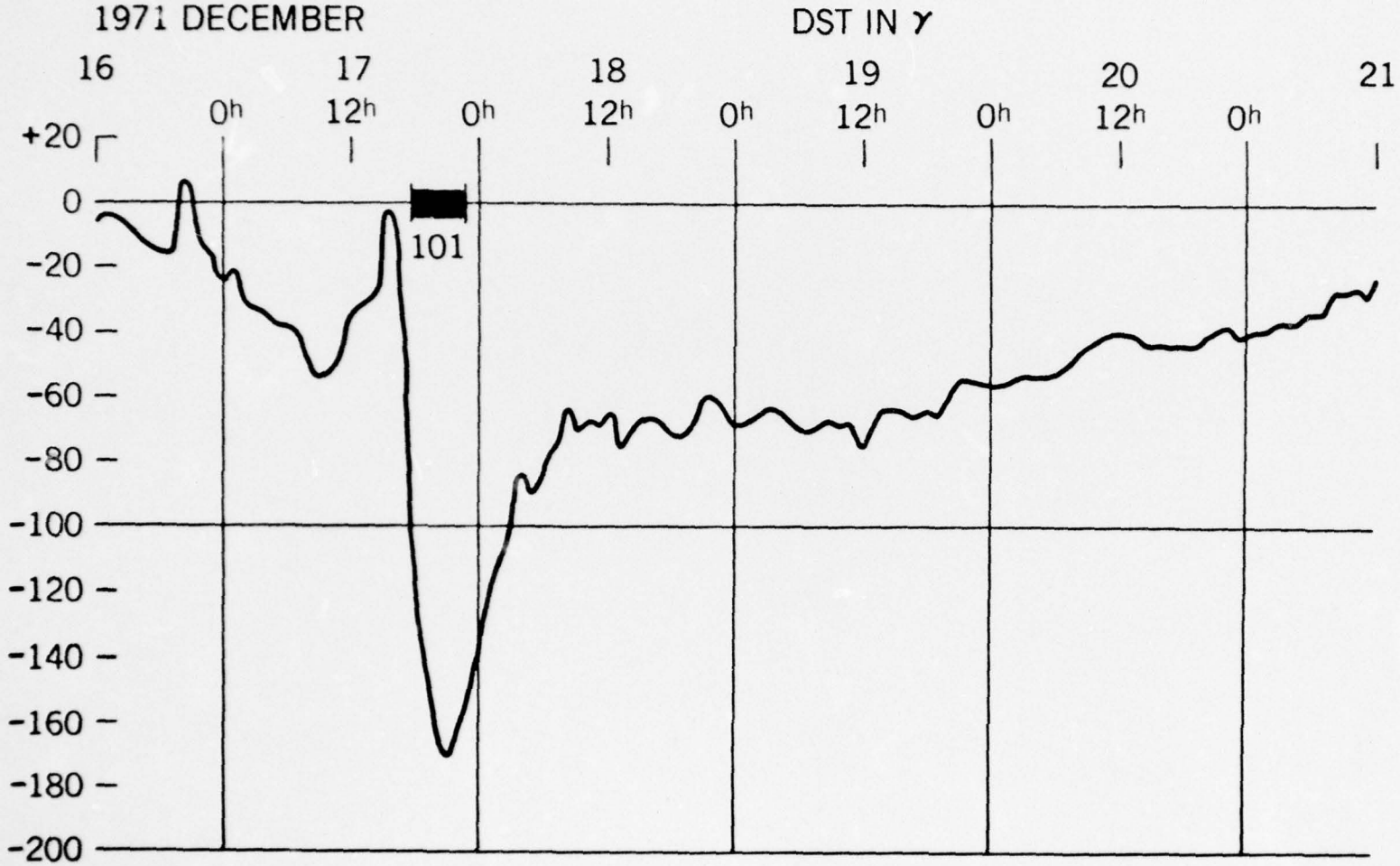
1971 DECEMBER
DST IN γ
16
17
18
19
20
21
0h
12h
0h
12h
0h
12h
0h
12h
0h
+20
0
-20
-40
-60
-80
-100
-120
-140
-160
-180
-200
101

Figure 12

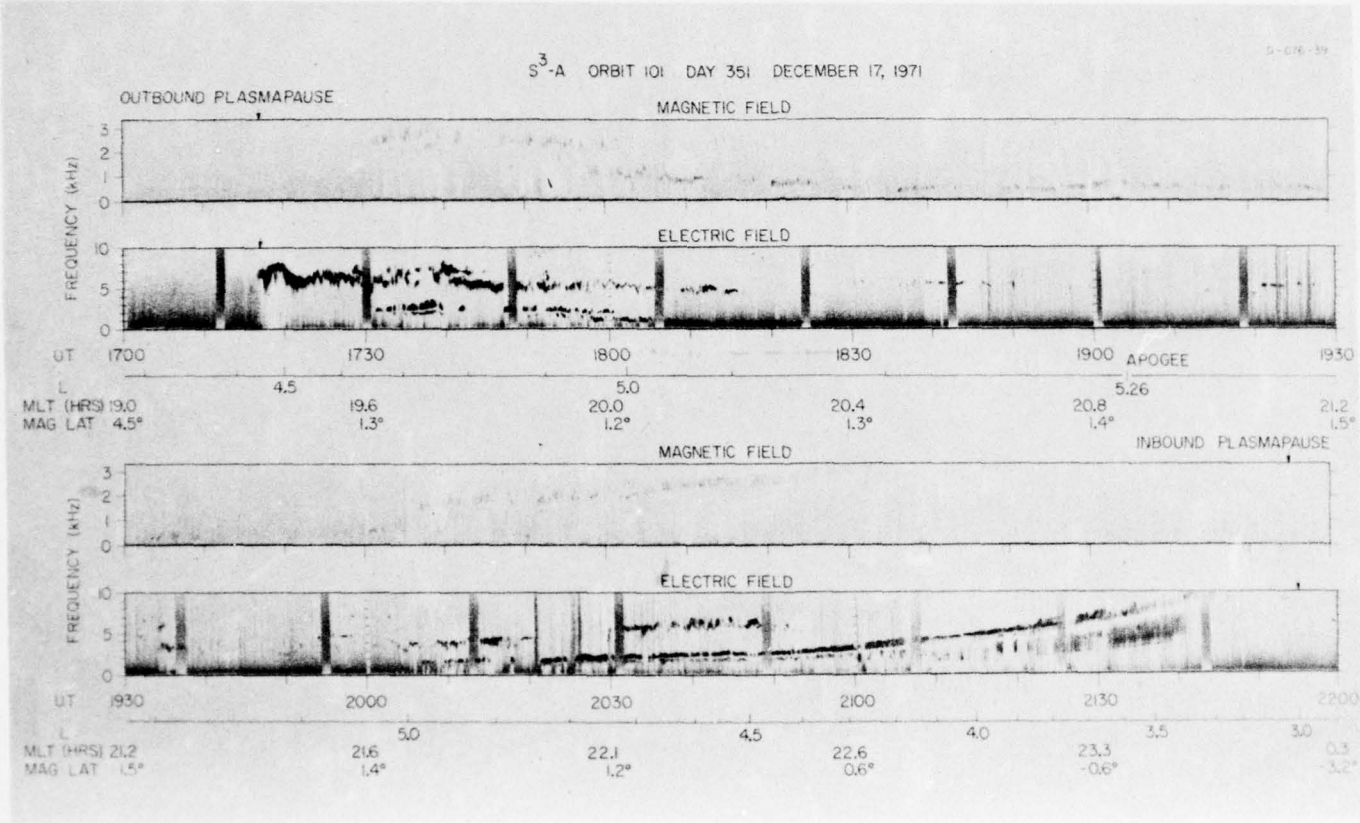
S3-A ORBIT 101 DAY 351 DECEMBER 17, 1971
OUTBOUND PLASMAPAUSE
MAGNETIC FIELD
ELECTRIC FIELD
FREQUENCY (kHz)
UT 1700 1730 1800 1830 1900 APOGEE 1930
L 4.5 5.0 5.26
MLT (HRS) 19.0 19.6 20.0 20.4 20.8 21.2
MAG LAT 4.5° 1.3° 1.2° 1.3° 1.4° 1.5°
INBOUND PLASMAPAUSE
MAGNETIC FIELD
ELECTRIC FIELD
FREQUENCY (kHz)
UT 1930 2000 2030 2100 2130 2200
L 5.0 4.5 4.0 3.5 3.0
MLT (HRS) 21.2 21.6 22.1 22.6 23.3 0.3
MAG LAT 1.5° 1.4° 1.2° 0.6° -0.6° -3.2°

Figure 13

A-G76-53

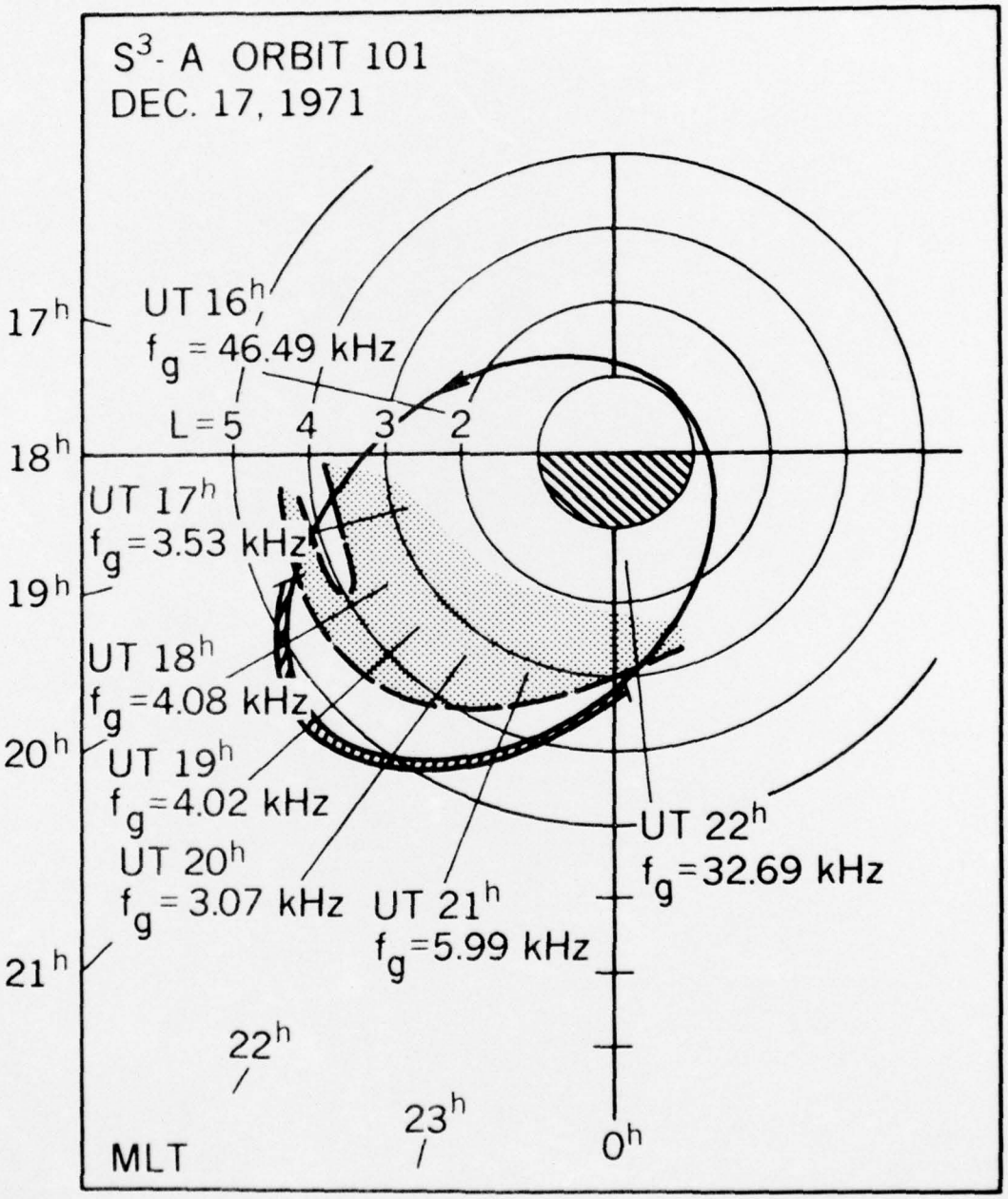

Figure 14

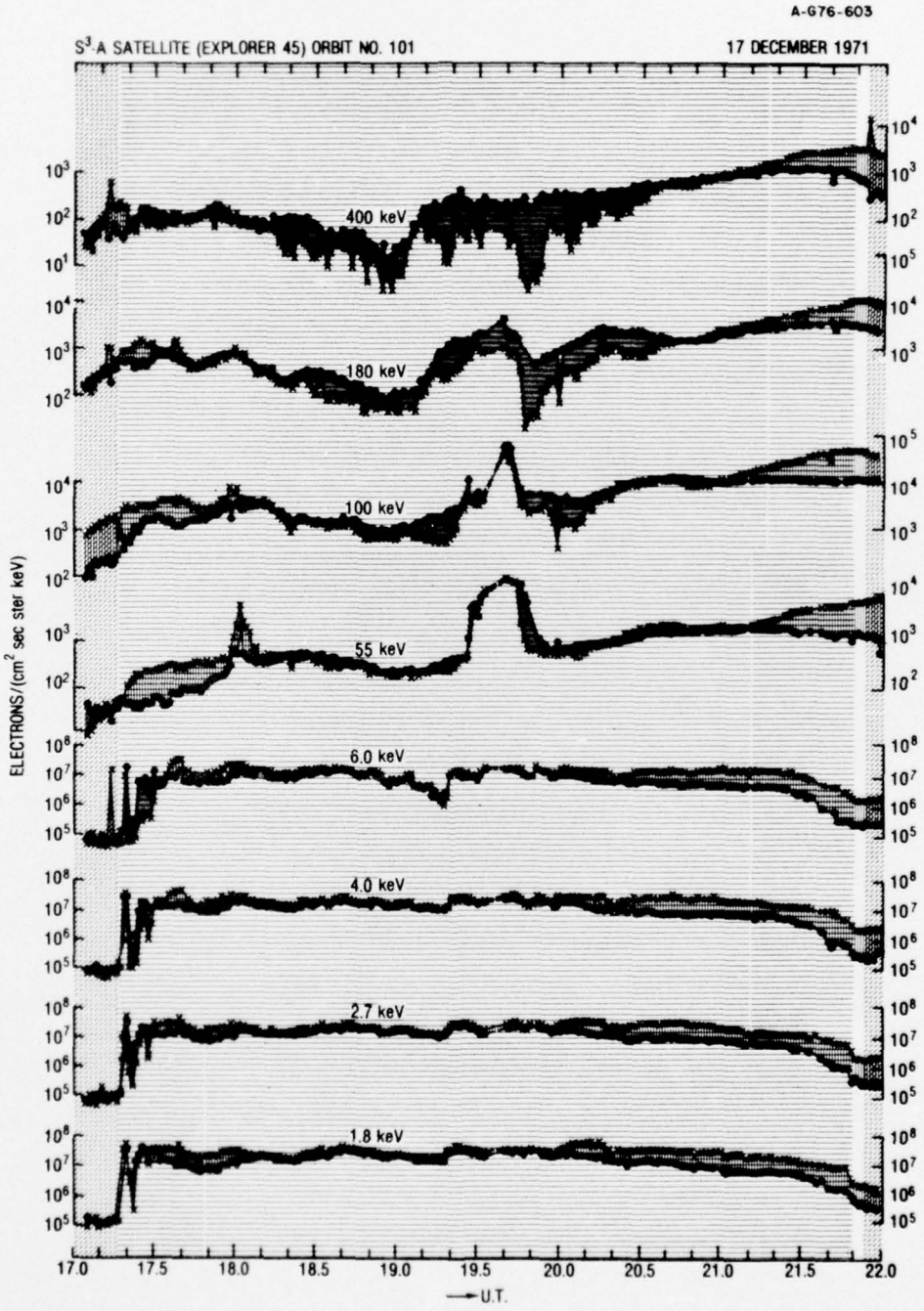
A-G76-603
S³-A SATELLITE (EXPLORER 45) ORBIT NO. 101
17 DECEMBER 1971
400 keV
180 keV
100 keV
55 keV
6.0 keV
4.0 keV
2.7 keV
1.8 keV
ELECTRONS/(cm² sec ster keV)
17.0
17.5
18.0
18.5
19.0
19.5
20.0
20.5
21.0
21.5
22.0
U.T.

Figure 15